

OAK RIDGE NATIONAL LABORATORY LIBRARIES



3 4456 0571525 0

ORNL-5404



Creep and Creep-Rupture Behavior of ERNiCr-3 Weld Metal

R. L. Klueh
J. F. King

This document does not contain UCNI, ECI, or other unclassified sensitive information and has been approved for release to the public by:

David R Hamrin 1/19/2010
David R. Hamrin, ORNL Classification Officer Date



OAK RIDGE NATIONAL LABORATORY
CENTRAL RESEARCH LIBRARY
CIRCULATION SECTION
4500N ROOM 175
LIBRARY LOAN COPY
DO NOT TRANSFER TO ANOTHER PERSON
If you wish someone else to see this report, send in name with report and the library will arrange a loan.
UCR 7962 - 9 77

OAK RIDGE NATIONAL LABORATORY
OPERATED BY UNION CARBIDE CORPORATION • FOR THE DEPARTMENT OF ENERGY

0 796 h 2

Printed in the United States of America. Available from
the Department of Energy,
Technical Information Center
P.O. Box 62, Oak Ridge, Tennessee 37830
Price: Printed Copy \$5.25; Microfiche \$3.00

This report was prepared as an account of work sponsored by an agency of the United States Government. Neither the United States Government nor any agency thereof, nor any of their employees, contractors, subcontractors, or their employees, makes any warranty, express or implied, nor assumes any legal liability or responsibility for any third party's use or the results of such use of any information, apparatus, product or process disclosed in this report, nor represents that its use by such third party would not infringe privately owned rights.

ORNL-5404
Distribution Category
UC-79b, -h, -k

Contract No. W-7405-eng-26

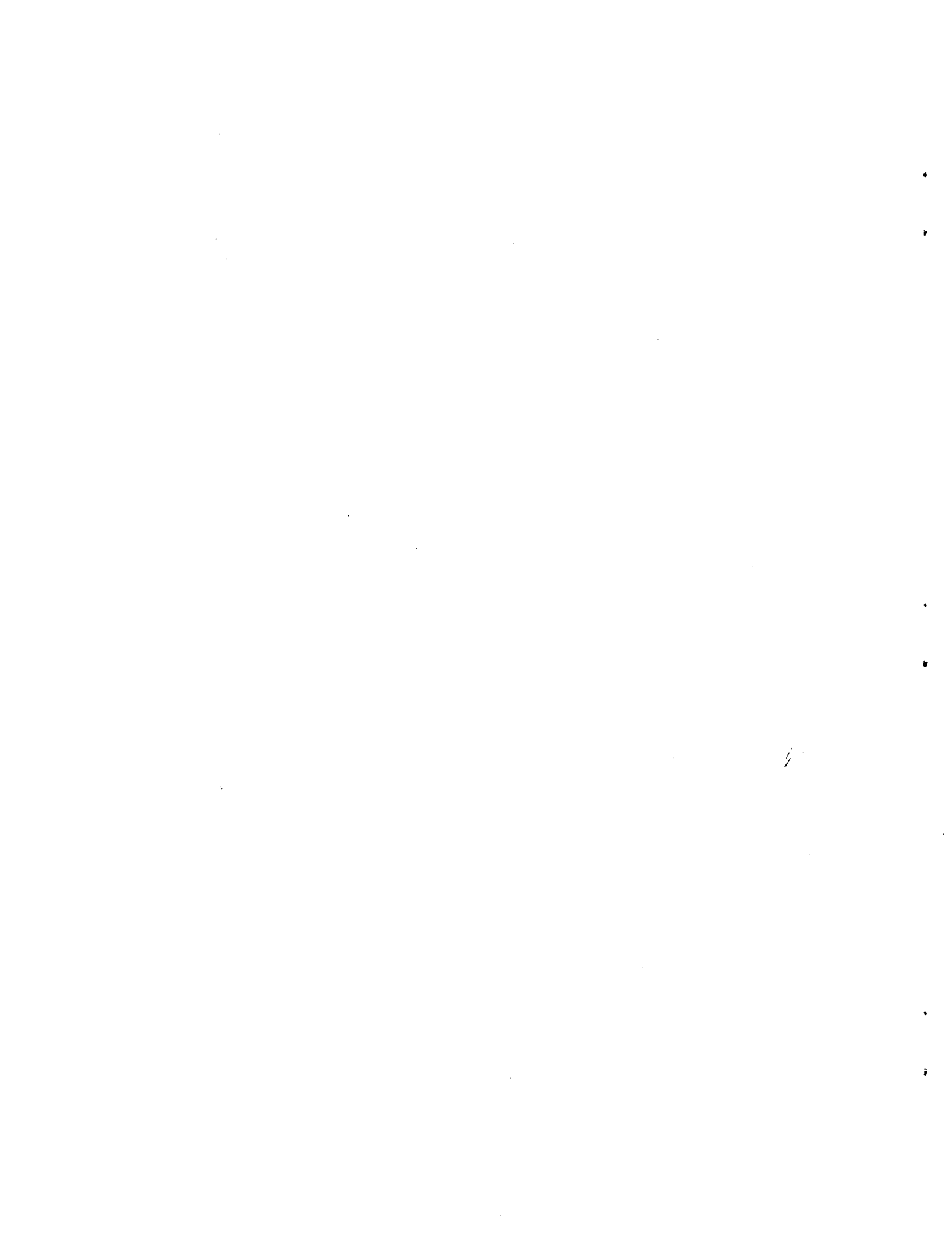
METALS AND CERAMICS DIVISION

CREEP AND CREEP-RUPTURE BEHAVIOR OF ERNiCr-3 WELD METAL

R. L. Klueh and J. F. King

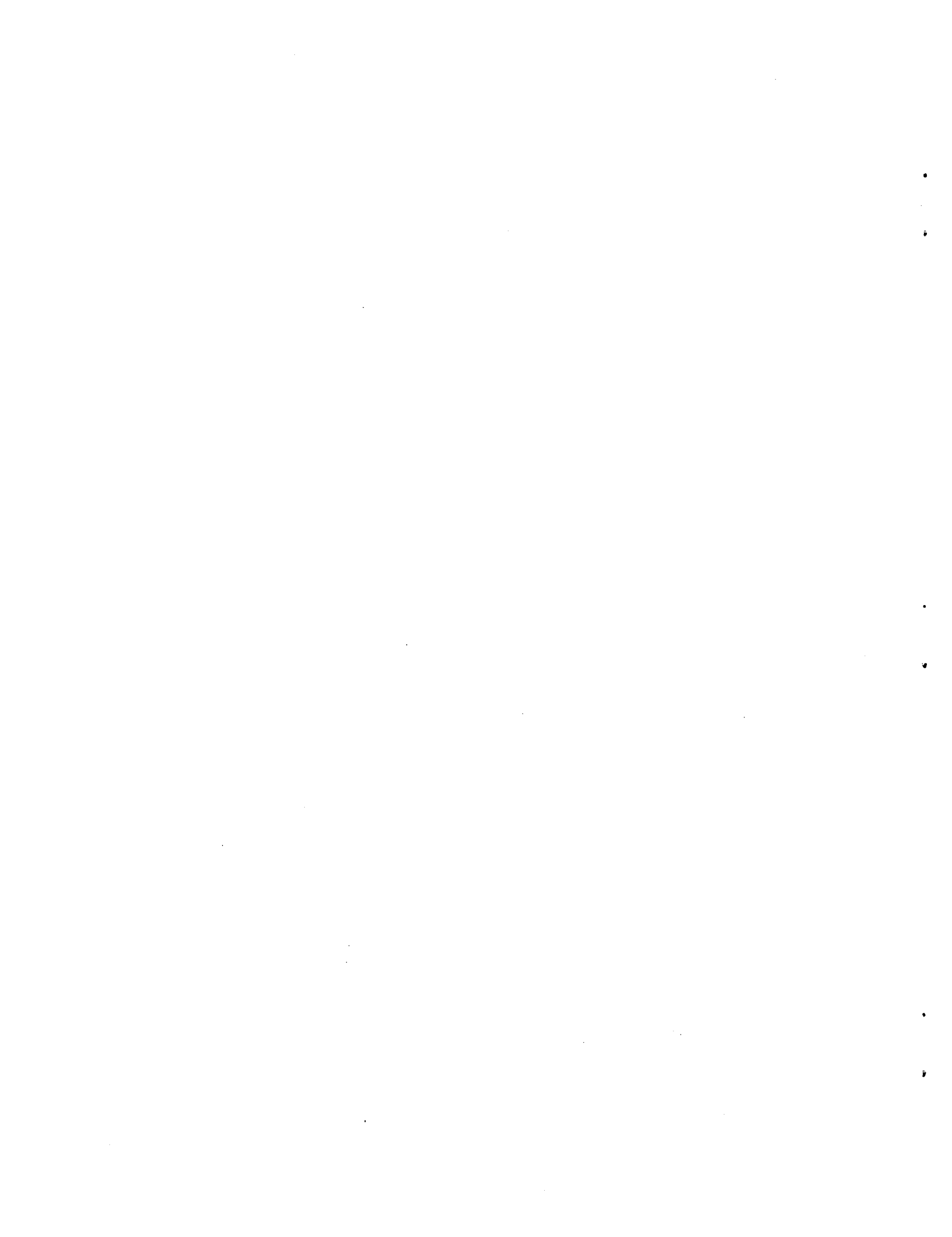
Date Published: June 1978

OAK RIDGE NATIONAL LABORATORY
Oak Ridge, Tennessee 37830
operated by
UNION CARBIDE CORPORATION
for the
DEPARTMENT OF ENERGY



CONTENTS

| | |
|-----------------------------------|----|
| ABSTRACT | 1 |
| INTRODUCTION | 1 |
| EXPERIMENTAL PROCEDURE | 3 |
| RESULTS | 4 |
| DISCUSSION | 24 |
| SUMMARY AND CONCLUSIONS | 39 |
| ACKNOWLEDGMENTS | 40 |
| REFERENCES | 40 |



CREEP AND CREEP-RUPTURE BEHAVIOR OF ERNiCr-3 WELD METAL*

7
R. L. Klueh and J. F. King

ABSTRACT

Creep and creep-rupture tests were made on AWS A5.14 Class ERNiCr-3 weld metal, commonly known as Inconel 82. Tests were made over the range 454–732°C on specimens taken from welds made by the gas tungsten-arc process. The results fell into two categories: those for tests at 454, 510, and 566°C displayed different characteristics than those at 621, 677, and 732°C. At the lower temperatures the creep curves were characterized by a rapid transient, a long steady-state stage, and little tertiary creep. At the elevated temperatures the transient stage was not as rapid, the steady-state creep stage was shorter, and the tertiary stage was longer. The low-temperature creep-rupture curves and stress-minimum creep rate curves were also much flatter than those at the elevated temperatures. For certain tests at 454, 510, and 566°C the creep curves exhibited an "instantaneous elongation" or "strain burst" phenomenon, in which the creep curves contained strain jumps. At these same temperatures, several specimens failed prematurely.

It was postulated that the strain bursts are related to the formation of dislocation pileups in the matrix. When a localized pileup breaks through a barrier, a dislocation avalanche results and triggers neighboring pileups. This process continues into neighboring grains and gives rise to the propagation of a deformation band along the gage length in a Luder's-type deformation. It was proposed that the premature failures were related to the strain burst phenomenon and some scattered "voids" or "cracks" that were observed in the as-welded microstructure.

INTRODUCTION

The nickel-base alloy with the American Welding Society designation AWS A5.14 Class ERNiCr-3 is a commonly used filler metal for joining several nickel-containing alloys using a variety of welding processes. Its nominal composition is as follows: 67% Ni, 20% Cr, 3% Mn, 2.5% Nb,

*Work performed under DOE/RRT 189a OH103, Piping and Fittings Development.

and lesser amounts of several other elements. This alloy, also known as Inconel 82, the trade name of Huntington Alloys, has found wide application as a filler metal for dissimilar-metal joining. Its widespread use for dissimilar-metal joints between austenitic stainless steel and ferritic steels makes it a prime candidate for use in the Clinch River Breeder Reactor (CRBR), where the intermediate loop piping to be constructed of type 316 stainless steel and the steam generators of 2 1/4 Cr-1 Mo steel.¹ Since welded transition joints between the austenitic and ferritic materials will be required, ERNiCr-3 has been chosen as the filler metal. Previous service experience with such joints in fossil-fired plants has caused sufficient concern that a program was initiated to improve the joint life expectancy.

Since the large thermal coefficient of expansion difference between 2 1/4 Cr-1 Mo steel and type 316 stainless steel can lead to large thermal stresses near the weld during thermal cycling, a transition piece is being considered to reduce these differences. In the proposed joint, Alloy 800H will be used as a spool piece, that is, 2 1/4 Cr-1 Mo steel will be welded to Alloy 800H, which will be welded to type 316 stainless steel. If such a transition piece is used, ERNiCr-3 filler metal would be used to join the Alloy 800H to the 2 1/4 Cr-1 Mo steel. The weld joint between type 316 stainless steel and Alloy 800H would probably be made with 16-8-2 filler metal. Since considerable data are available for 16-8-2 weld metal, our first mechanical properties studies dealt with ERNiCr-3.

We previously published data on the tensile properties of ERNiCr-3 weld metal.² Few creep data are available in the literature: Payne³ gives 100, 1000, and 10000-hr rupture stresses at 540, 650, 760, 870, and 980°C, but gives no actual experimental results. The only other known creep data are unpublished proprietary creep-rupture data of Huntington Alloys,⁴ data to which we have had access. The Huntington Alloys data are usually in the form of two to three data points — enough to establish a rupture curve and estimate stresses for rupture in 10,000 hr — at 538, 649, 760, and 871°C. No data are available at the temperatures applicable to the operation of the transition joint — near 510°C.

EXPERIMENTAL PROCEDURE

Two types of welds were made. The first was made between two 13-mm-thick (0.50-in.) plates — one plate of 2 1/4 Cr-1 Mo steel and the other of Alloy 800H. A 90°-included-angle V-groove geometry was used, requiring a root pass and seven fill passes. Since very few specimens could be obtained from such a small weld, a larger weld geometry was designed. Plates of 19-mm-thick (0.75-in.) 2 1/4 Cr-1 Mo steel were welded with a 30°-included-angle V-groove joint geometry with a 32-mm (1.25-in.) root opening and a backing strip. To fill this joint, 40 weld passes were required. In both cases the welding was performed by the automatic gas tungsten-arc process with cold-wire filler additions. The nominal welding parameters were: 150 A and 10 V with a travel speed of about 0.9 mm/s. In Table 1 the chemical composition of a large and a small weld are given, as well as the American Welding Society (AWS) and American Society for Testing and Materials (ASTM) specification for ERNiCr-3. Because of base metal dilution, the small weld contained more than the allowable iron concentration.

Table 1. Chemical Composition of
ERNiCr-3 Filler Metal

| Element | Chemical Composition, wt % | | |
|---------|----------------------------|-------------------|-------------------------|
| | Small Weldment | Large Weldment | ASTM B.304 AWS A5.14 |
| Ni | Balance | Balance | 67.0 min |
| Cu | | 0.3 | 0.5 max |
| Mn | 2.7 | 2.0 | 2.5-3.5 |
| Fe | 10 | 2.8 | 3.0 max |
| Si | | 0.2 | 0.5 max |
| C | 0.03 | 0.02 | 0.1 max |
| S | | | 0.015 max |
| Ti | 0.3 | 0.41 | 0.75 max |
| Nb | 1.8 | 1.8 | 2.0-3.0 |
| Cr | 18.0 | 19.5 | 18-22 |

All welds were radiographed, and no defects were detected. Because of several premature creep failures early in the program, all subsequent specimens were radiographed before testing. Only a few specimens were found to contain defects, none of which were large enough to warrant rejecting the weld. Specimens that contained defects were not tested.

The creep-rupture test specimens were a buttonhead type with a 3.18-mm-diam (0.125-in.) and 28.6-mm-long (1.125-in.) gage section. The specimens tested were longitudinal all-weld-metal specimens. Before test, all specimens were given a 1-hr postweld heat treatment at 732°C.

Creep-rupture tests were made at 454, 510, 566, 621, 677, and 732°C in air in constant-load lever-arm creep frames. During test the specimens were heated in a resistance tube furnace, and the temperature was monitored and controlled by three Chromel-P-Alumel thermocouples attached to the specimen gage length. Temperature was controlled to $\pm 1^\circ\text{C}$, the temperature along the gage length varying less than $\pm 2^\circ\text{C}$. Elongations were determined with mechanical extensometers attached to the specimen grips, and the specimen elongation was read periodically on a dial gage.

RESULTS

Creep-rupture tests were made at 454, 510, 566, 621, 677, and 732°C. The first tests were made at 510 and 566°C on specimens taken from the smaller weldments (seven-pass welds made on 13-mm-thick plates). Because only a few specimens could be obtained from the smaller weldments, later tests were made on specimens taken from the large weldments (forty-pass welds on 19-mm-thick plates). The effect of the weldment size on the tensile properties was previously investigated;² the effects that this could have on the creep-rupture properties will be discussed below. Several specimens tested at 454, 510, and 566°C failed prematurely. Although the results of these tests are given in Table 2, they are not included in the graphical presentations of the data.

The creep and rupture behavior were quite temperature-dependent. For that reason the results are presented in two tables: Tables 2 and 3, respectively, show the data for tests at and below 566°C. Logarithmic plots of stress against rupture life (Fig. 1) and stress against minimum

Table 2. Creep-Rupture Properties of ERNiCr-3 Weld Metal at 454, 510, and 566°C

| Stress | | Rupture | Total | Reduction | Minimum | Loading |
|--|--------------------------|---------------------------|----------------|-------------|-------------------|------------|
| (MPa) | (ksi) | Life (hr) | Elongation (%) | of Area (%) | Creep Rate (%/hr) | Strain (%) |
| <u>Tests at 454°C (850°F) on Welds in 19-mm (3/4-in.) Plate</u> | | | | | | |
| 414 | 60.0 | <i>a</i> | | | 0.0000140 | 8.4 |
| 434 | 63.0 | <i>a</i> | | | 0.0000318 | 11.7 |
| 455 | 66.0 | <i>a</i> | | | 0.000090 | 13.5 |
| 483 | 70.0 | <i>b</i> | | | 0.000273 | 13.9 |
| 483 | 70.0 | 68.1 ^{<i>c</i>} | 37.0 | 54.2 | 0.00769 | 23.7 |
| 483 | 70.0 | 75.1 ^{<i>c</i>} | 33.4 | 50.5 | 0.0187 | 22.4 |
| 489 | 71.0 | 1075.4 | 33.2 | 55.2 | 0.00063 | 19.8 |
| 496 | 72.0 | 1012.6 | 36.0 | 38.5 | 0.000938 | 24.3 |
| 496 | 72.0 | 715.1 ^{<i>c</i>} | 40.1 | 41.7 | 0.00207 | 27.0 |
| 510 | 74.0 | 142.3 | 40.2 | 52.5 | 0.0130 | 29.5 |
| 517 | 75.0 | 3.2 | 33.7 | 53.0 | 0.125 | 26.3 |
| <u>Tests at 510°C (950°F) on Welds in 13-mm (1/2-in.) Plate</u> | | | | | | |
| 379 | 55.0 | 6770.4 | 15.7 | 15.2 | 0.0000187 | 10.4 |
| 396 | 57.5 | 3255.0 | 11.5 | 15.6 | 0.0000440 | 6.7 |
| 414 | 60.0 | 1645.4 | 23.6 | 19.7 | 0.000463 | 17.3 |
| 434 | 63.0 | 1205.1 | 33.7 | 29.3 | 0.000536 | 24.9 |
| 448 | 65.0 | 357.1 | 39.1 | 35.9 | 0.00459 | 29.4 |
| 455 | 66.0 | 4.0 ^{<i>c</i>} | 40.4 | 39.0 | 0.150 | 31.3 |
| 455 | 66.0 | 39.4 | 38.7 | 42.9 | 0.138 | 26.5 |
| 465 | 67.5 | 37.1 ^{<i>c</i>} | 48.4 | 51.8 | 0.209 | 33.9 |
| 483 | 70.0 | 10.9 | 48.4 | 53.7 | 0.395 | 33.6 |
| <u>Tests at 566°C (1050°F) on Welds in 13-mm (1/2-in.) Plate</u> | | | | | | |
| 328 | 47.5 | <i>a</i> | | | 0.0000149 | 5.8 |
| 345 | 50.0 | 778.8 ^{<i>c</i>} | 14.5 | 15.6 | 0.000324 | 8.5 |
| 345 | 50.0 ^{<i>d</i>} | 6003.3 | 8.3 | 6.4 | 0.0000330 | 5.0 |
| 365 | 53.0 | 1087.5 | 17.2 | 18.2 | 0.000611 | 11.6 |
| 379 | 55.0 | 841.1 | 18.9 | 18.9 | 0.00105 | 12.0 |
| 396 | 57.5 | 448.2 | 21.4 | 19.6 | 0.00280 | 14.2 |
| 396 | 57.5 ^{<i>d</i>} | 124.6 ^{<i>c</i>} | 21.9 | 25.6 | 0.0652 | 8.5 |
| 396 | 57.5 ^{<i>d</i>} | 63.8 ^{<i>c</i>} | 22.2 | 30.9 | 0.133 | 9.6 |
| 414 | 60.0 | 112.8 | 29.7 | 27.4 | 0.0331 | 18.7 |
| 434 | 63.0 | 29.5 | 37.6 | 36.8 | 0.231 | 24.5 |

^{*a*}Test discontinued before rupture.

^{*b*}Temperature overshoot and test failed after 2430 hr.

^{*c*}Premature failure.

^{*d*}Tests made on 19-mm (3/4-in.) plate.

Table 3. Creep-Rupture Properties of ERNiCr-3 Weld Metal at 621, 677, and 732°C^a

| Stress | | Rupture Life (hr) | Total Elongation (%) | Reduction of Area (%) | Minimum Creep Rate (%/hr) | Loading Strain (%) |
|--------------------------------|-------|-------------------|----------------------|-----------------------|---------------------------|--------------------|
| (MPa) | (ksi) | | | | | |
| <u>Tests at 621°C (1150°F)</u> | | | | | | |
| 241 | 35.0 | 3109.4 | 5.3 | 5.4 | 0.000843 | 0.11 |
| 276 | 40.0 | 1195.9 | 6.7 | 14.8 | 0.00321 | 0.28 |
| 293 | 42.5 | 653.1 | 10.8 | 16.8 | 0.00973 | 0.61 |
| 310 | 45.0 | 295.1 | 14.1 | 39.7 | 0.0251 | 0.63 |
| 379 | 55.0 | 21.2 | 25.4 | 33.7 | 0.660 | 3.63 |
| <u>Tests at 677°C (1250°F)</u> | | | | | | |
| 138 | 20.0 | 3590.0 | 8.6 | 9.2 | 0.000312 | 0.23 |
| 172 | 25.0 | 778.5 | 15.0 | 27.9 | 0.00436 | 0.23 |
| 207 | 30.0 | 215.0 | 17.7 | 30.8 | 0.0220 | 0.28 |
| 241 | 35.0 | 89.0 | 25.2 | 39.7 | 0.080 | 0.41 |
| 276 | 40.0 | 26.0 | 33.4 | 49.1 | 0.326 | 0.41 |
| <u>Tests at 732°C (1350°F)</u> | | | | | | |
| 83 | 12.0 | 2792.8 | 13.5 | 24.0 | 0.000352 | 0.13 |
| 103 | 15.0 | 634.4 | 23.2 | 23.2 | 0.00380 | 0.21 |
| 138 | 20.0 | 103.6 | 26.8 | 50.0 | 0.0603 | 0.42 |
| 172 | 25.0 | 30.7 | 41.8 | 40.6 | 0.342 | 0.46 |

^aAll specimens were taken from welds made in 19-mm-thick plate.

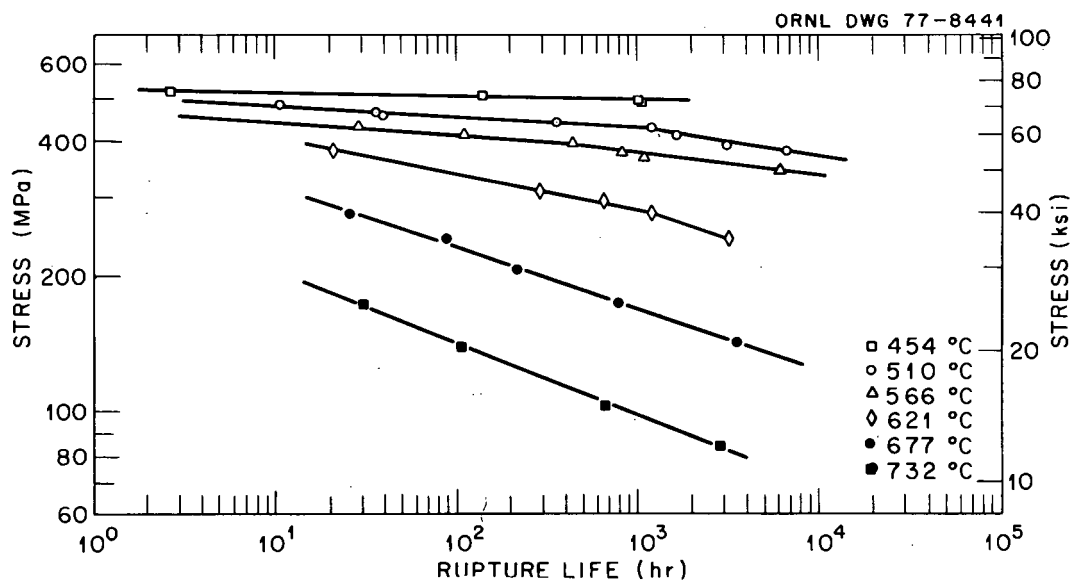


Fig. 1. Creep-Rupture Curves for ERNiCr-3 (Inconel 82) Weld Metal.

creep rate (Fig. 2) indicate a distinct difference in behavior for the two temperature regimes. At the higher stresses and at 454, 510, and 566°C, the curves (Figs. 1 and 2) are quite flat. At 510 and 566°C, there appeared to be changes in slope (it breaks downward) as the stress was lowered. At these temperatures the curves for rupture life (Fig. 1) and minimum creep rate (Fig. 2) both show such breaks. At 454°C, however, only the minimum creep rate curve breaks downward; that is, sufficient rupture-life data were not obtained to determine the break.

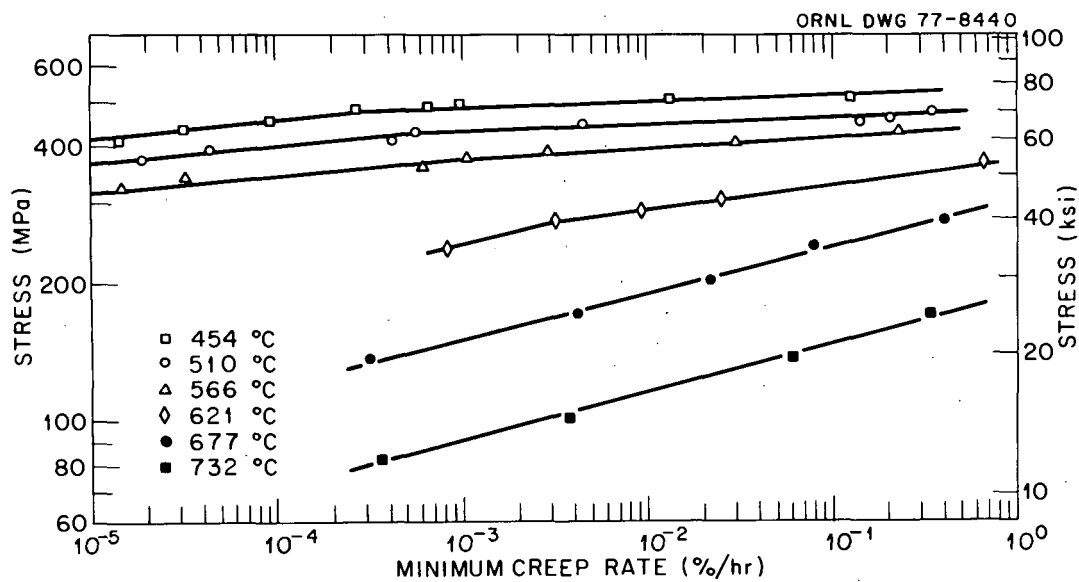


Fig. 2. Relationship Between Stress and Minimum Creep Rate for ERNiCr-3 (Inconel 82) Weld Metal.

The rupture-life data at the high temperatures — 621, 677, and 732°C — have a different character. At 677 and 732°C a single straight line appears to fit the data. Although more data are required to confirm the interpretation, at 621°C the curves appear to break downward. The minimum creep rate data (Fig. 2) show this more clearly than the rupture life data (Fig. 1) do. However, the high-stress end of the 621°C curves was not as flat as the low-temperature curves.

Creep rate data (Fig. 2) are generally fit by a power law equation of the type

$$\dot{\epsilon} = A\sigma^n, \quad (1)$$

where σ is the stress, $\dot{\epsilon}$ the minimum creep rate, and A and n are constants. To characterize the data better, we estimated n for the data in Fig. 2 (Table 4). It should be noted that these are but rough estimates based on the visual fit of the data.

The estimated n values again reveal the difference in behavior at low and high temperatures. At 621, 677, and 732°C, the high-temperature regime, n is between 8 and 10. For the data at 621°C, which were judged to have a break in the curve, this value applied at low stresses. The low-stress and low-temperature data curves all had n values between 24 and 28. At the high stresses, very large n values were calculated.

Table 4. Estimated Stress Exponents for the Creep of ERNiCr-3

| Temperature (°C) | Estimated Transition Stress, ^a (MPa) | Stress Exponent, n | |
|---------------------|--|----------------------|------------|
| | | High Stress | Low Stress |
| 454 | 480 | 66 | 24 |
| 510 | 430 | 70 | 28 |
| 566 | 380 | 45 | 28 |
| 621 | 270 | 18 | 9.6 |
| 677 | | | 7.8 |
| 732 | | | 8.6 |

^aTransition between high-stress and low-stress regimes.

Another indication of the difference in behavior at the high and low temperatures is seen by comparing the creep curves at the various temperatures (Figs. 3 and 4). At the low temperatures (Fig. 3), and especially at low stresses, the curves are characterized by a high initial creep rate followed by a rapid transient during which the creep rate decreases to a "steady state." As discussed in the following section, the low-stress tests — especially at 454°C — may follow a logarithmic creep law, which implies a continuously decreasing creep rate. Once the steady state is reached, it continues almost to failure. That is, these tests showed essentially no tertiary creep. At the highest stresses the transition from the primary to the secondary stage was less abrupt.

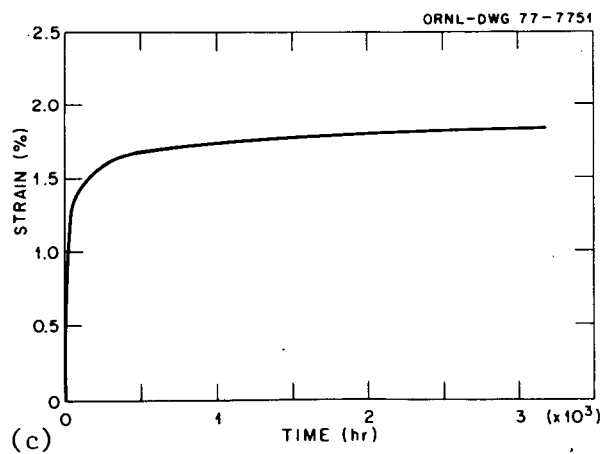
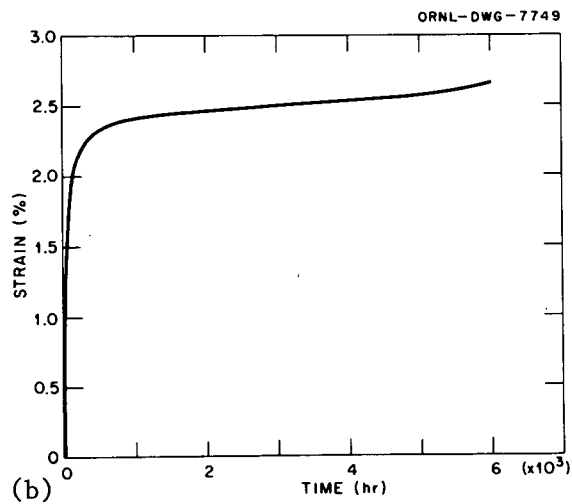
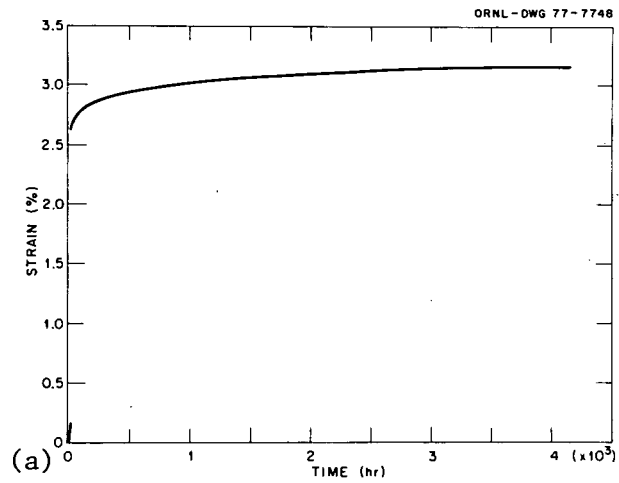


Fig. 3. Example of Creep-Curve Shape at (a) 454°C and 413 MPa; (b) 510°C and 327 MPa; (c) 566°C and 327 MPa. Only the early portion of each curve is shown.

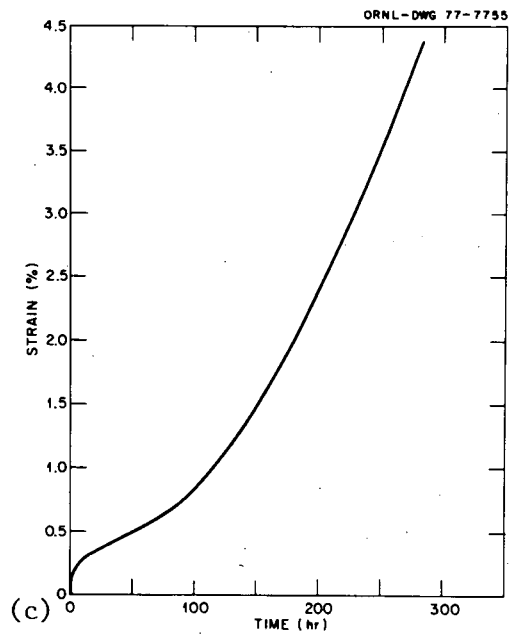
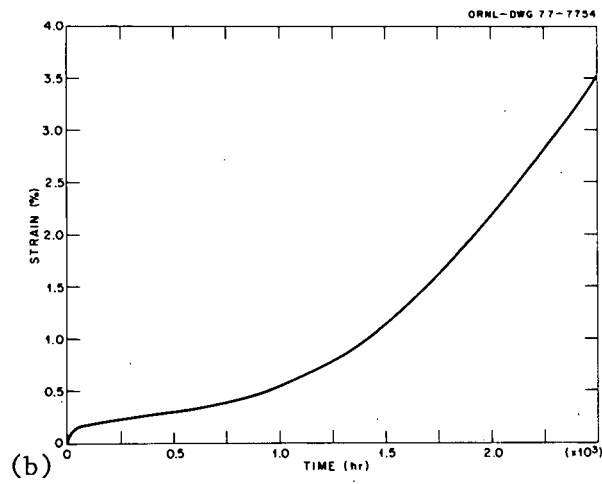
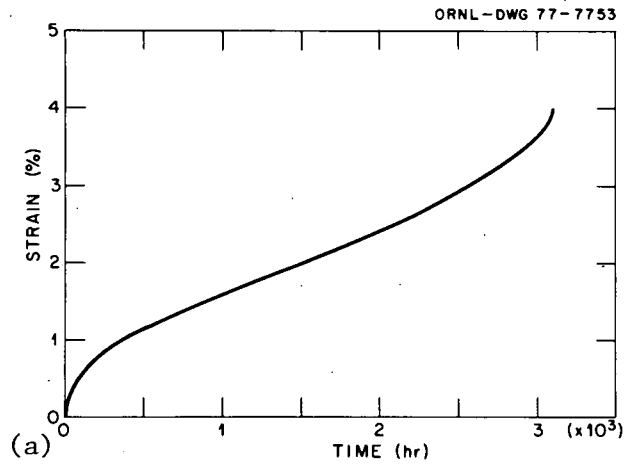


Fig. 4. Example of Creep-Curve Shape at (a) 621°C and 241 MPa; (b) 677°C and 138 MPa; (c) 732°C and 103 MPa. Only the early portion of each curve is shown.

At the two highest temperatures, 677 and 732°C, the creep curves are characterized by very little primary creep [Fig. 4(b) and (c)]. The test quickly reached the steady-state stage, which was also shorter than it was at the lower temperatures. These curves have well-defined tertiary stages. Finally, the curve shapes at 621°C [Fig. 4(a)] appear to fall between those at the low temperatures (Fig. 3) and those at 677 and 732°C [Figs. 4(b) and (c)]. The transition to the steady state occurred over a longer period of time and with more strain than had occurred at 677 and 732°C. Furthermore, the initial creep rate was lower and the transition to the steady-state creep rate was more gradual than in the low-temperature tests.

The characteristic shapes of the creep curves are further demonstrated by comparing the tertiary creep behavior at the different temperatures (Table 5). For numerous alloys the time to tertiary creep, t_2 , is related to the rupture life, t_R , according to

$$t_2 = At_R^\alpha, \quad (2)$$

where A and α are constants; ⁵⁻⁷ α is very often equal to unity, making the ratio t_2/t_R a constant. Values for this ratio for ERNiCr-3 weld metal were determined (Tables 4 and 5).

As stated above, the tests at the low temperatures showed essentially no tertiary creep. This is reflected in the ratio t_2/t_R at 454, 510, and 566°C (Table 5): the ratio is always greater than 0.92, and with a few exceptions, always greater than or equal to 0.97. The exceptions occurred for short-time tests, in which a lack of data made it difficult to estimate t_2 . Although strains to tertiary creep for these tests were quite scattered, they tended to decrease with decreasing stress (increasing rupture life).

At the two highest temperatures, 677 and 732°C, the tertiary creep behavior differed considerably from that at the lower temperatures: here t_2/t_R was much smaller. While it approached 0.99 at the lower temperatures, it approached 0.15 at 677 and 732°C. Strains to tertiary creep were considerably less, but they also decreased with decreasing stress. The results at 621°C fell between those at the lower and higher temperatures,

Table 5. Time and Strain to Tertiary Creep of ERNiCr-3 Filler Metal

| Stress | | Time, hr | | Strain to Tertiary (%) | Ratio t_2/t_R |
|--------------------------------|-------------------|------------|-------------|------------------------|-----------------|
| (MPa) | (ksi) | To Rupture | To Tertiary | | |
| <u>Tests at 454°C (850°F)</u> | | | | | |
| 414 | 60.0 | <i>a</i> | | | |
| 434 | 63.0 | <i>a</i> | | | |
| 455 | 66.0 | <i>a</i> | | | |
| 483 | 70.0 | <i>b</i> | | | |
| 483 | 70.0 | 68.1 | 67 | 8.8 | 0.98 |
| 483 | 70.0 | 75.1 | 74 | 2.7 | 0.99 |
| 489 | 71.0 | 1075.4 | 1070 | 9.7 | 0.99 |
| 496 | 72.0 | 1012.6 | 1000 | 8.9 | 0.99 |
| 510 | 74.0 | 142.3 | 141 | 2.8 | 0.99 |
| 517 | 75.0 | 3.2 | 3 | 2 | 0.94 |
| <u>Tests at 510°C (950°F)</u> | | | | | |
| 379 | 55.0 | 6770.4 | 6750 | 2.8 | >0.99 |
| 396 | 57.5 | 3255.0 | 3250 | 3.9 | >0.99 |
| 414 | 60.0 | 1645.4 | 1635 | 6.6 | 0.99 |
| 434 | 63.0 | 1205.1 | 1200 | 7.2 | >0.99 |
| 448 | 65.0 | 357.1 | 350 | 4.3 | 0.98 |
| 455 | 66.0 | 4.0 | | | |
| 455 | 66.0 | 39.4 | 37 | 6.0 | 0.94 |
| 465 | 67.5 | 37.1 | 36 | 12.9 | 0.97 |
| 483 | 70.0 | 10.9 | 10 | 13.9 | 0.92 |
| <u>Tests at 566°C (1050°F)</u> | | | | | |
| 328 | 47.5 | <i>a</i> | | | |
| 345 | 50.0 | 778.8 | 770 | 4.7 | 0.99 |
| 345 | 50.0 | 6003.3 | 5995 | 2.2 | 0.99 |
| 365 | 53.0 | 1087.5 | 1070 | 4.6 | 0.98 |
| 379 | 55.0 | 841.1 | 835 | 5.9 | 0.99 |
| 396 | 57.5 | 448.2 | 445 | 6.4 | 0.99 |
| 396 | 57.5 ^c | 124.6 | 121 | 12.0 | 0.97 |
| 396 | 57.5 ^c | 63.8 | 63 | 11.9 | 0.99 |
| 414 | 60.0 | 112.8 | 110 | 9.8 | 0.98 |
| 434 | 63.0 | 29.5 | 28 | 11.5 | 0.95 |
| <u>Tests at 621°C (1150°F)</u> | | | | | |
| 241 | 35.0 | 3109.4 | 2825 | 3.3 | 0.91 |
| 276 | 40.0 | 1195.9 | 1170 | 5.3 | 0.98 |
| 293 | 42.5 | 653.1 | 735 | 8.9 | 0.97 |
| 310 | 45.0 | 295.1 | 288 | 11.8 | 0.98 |
| 379 | 55.0 | 21.2 | 8 | 6.2 | 0.38 |
| <u>Tests at 677°C (1250°F)</u> | | | | | |
| 138 | 20.0 | 3590.0 | 1150 | 0.7 | 0.32 |
| 172 | 25.0 | 778.5 | 100 | 0.8 | 0.13 |
| 207 | 30.0 | 215.0 | 33 | 1.0 | 0.15 |
| 241 | 35.0 | 89.0 | 15 | 1.5 | 0.17 |
| 276 | 40.0 | 26.0 | 3.3 | 1.4 | 0.13 |
| <u>Tests at 732°C (1350°F)</u> | | | | | |
| 83 | 12.0 | | | | |
| 103 | 15.0 | 634.4 | 105 | 0.9 | 0.17 |
| 138 | 20.0 | 103.6 | 15 | 1.3 | 0.14 |
| 172 | 25.0 | 30.7 | 3.5 | 1.5 | 0.11 |

^a Test discontinued before rupture.

^b Temperature overshoot and test failed after 2430 hr.

^c Test made on 19-mm (3/4 in.) plate.

but most resembled the results at the lower temperatures: for most tests, t_2/t_R exceeded 0.9; the strains to tertiary creep were larger than they were at 677 and 732°C, and decreased with decreasing stress.

In general the total elongations and reductions of area were consistent at all temperatures (Figs. 5 and 6). Except at 454°C, both decreased with decreasing stress (increasing rupture life). At 454°C ductility changed very little over the range of stresses tested. Interestingly, of the high-temperature tests (Fig. 6), those at 621°C showed the least elongation.

As stated above several specimens ruptured prematurely at 454, 510, and 566°C. We also noted another peculiarity at these temperatures: it can be described as an "instantaneous elongation," a "strain burst,"

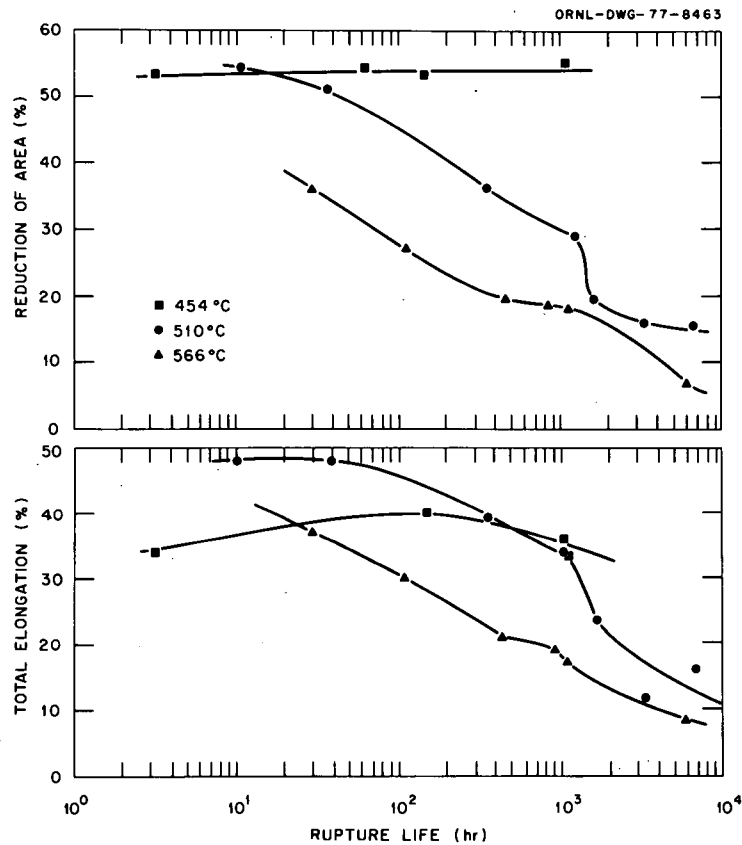


Fig. 5. Total Elongation and Reduction of Area as Functions of Rupture Life for ERNiCr-3 (Inconel 82) Weld Metal at 454, 510, and 566°C. Data points were connected to indicate the trends.

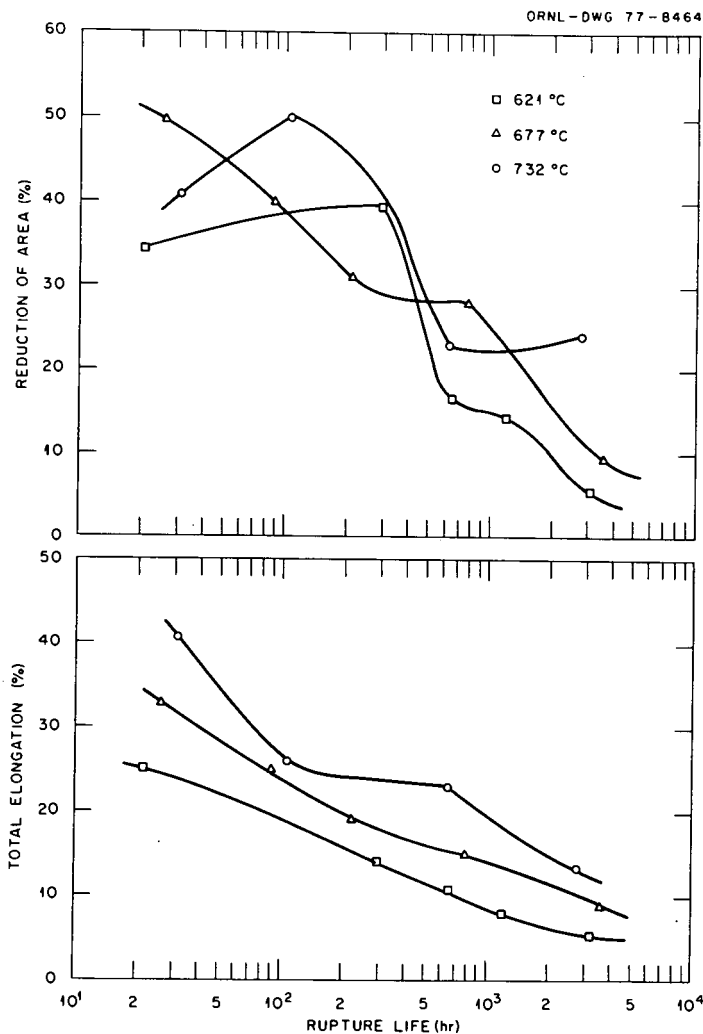


Fig. 6. Total Elongation and Reduction in Area as Functions of Rupture Life for ERNiCr-3 (Inconel 82) Weld Metal at 621, 677, and 732°C. Data points were joined to indicate the trends.

or a "spontaneous deformation." The phenomenon exhibited itself in the form of a jump in the creep curves, examples of which are shown in Figs. 7-9. These "strain bursts" appeared at different times in the creep process: shortly after loading during primary creep (Fig. 7) and during secondary creep (Fig. 8). Single (Fig. 8) and multiple (Fig. 9) bursts were observed. When a burst occurred early in the creep test (Fig. 7), it was difficult to determine whether there was a single or multiple burst.

The phenomenon was quite general at 454 and 510°C, where essentially all tests displayed one or more strain bursts. Only a few tests displayed

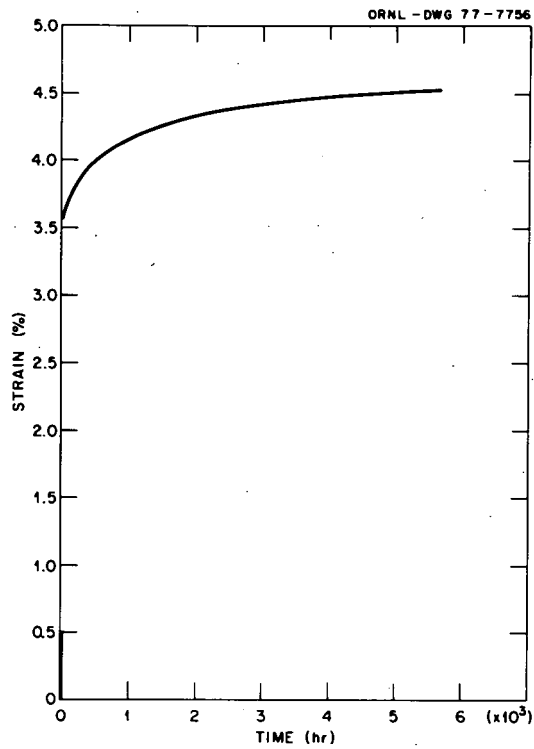


Fig. 7. Example of "Instantaneous Elongation" or a "Strain Burst" During Primary Creep in ERNiCr-3 Weld Metal Tested at 454°C and 434 MPa.

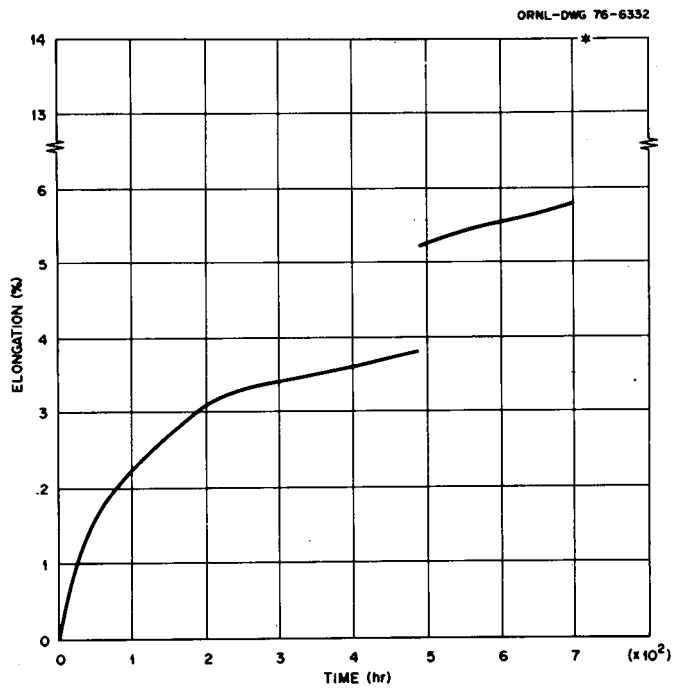


Fig. 8. Example of a "Strain Burst" During Secondary Creep Stage of ERNiCr-3 Weld Metal Tested at 454°C and 496 MPa.

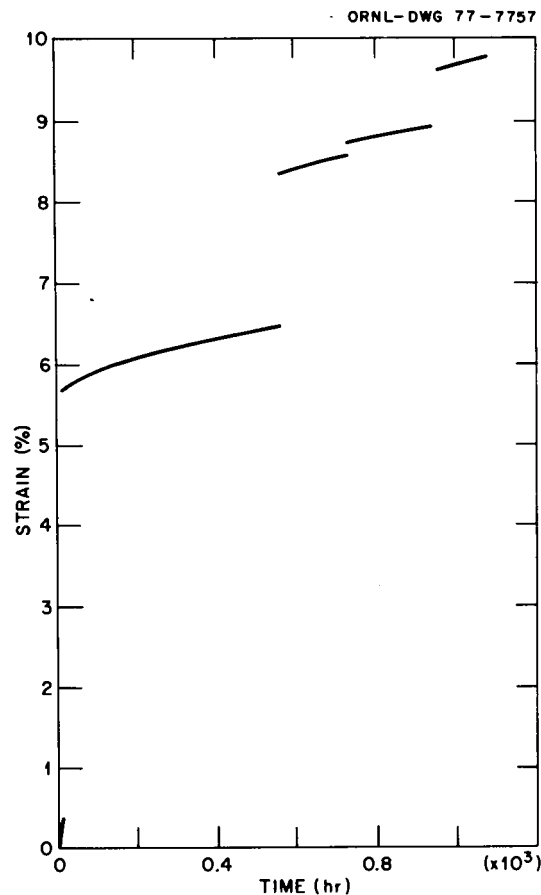


Fig. 9. Example of Multiple "Strain Bursts" in ERNiCr-3 Weld Metal Tested at 454°C and 489 MPa.

the phenomenon at 566°C, and no strain bursts were seen at 621, 677, and 732°C. The estimated strains per burst are given in Table 6. Strain burst magnitudes ranged from strains of about 0.1% to greater than 6%. When the strain burst occurred during the steady-state stage, the creep rate after the burst was usually little different than before it (Fig. 9).

No direct evidence exists to link the strain burst phenomenon with the observations of premature failure. However, the fact that both phenomena occurred only in the low-temperature tests could signify a relationship. It is as if a premature failure occurred during a strain burst larger than the ductility of the alloy could absorb. The difficulty in relating strain bursts to premature failures was evident when the three tests made at 454°C and 428 MPa (70 ksi) were examined (Table 2).

Table 6. Strain Burst Observations on ERNiCr-3
at 454, 510, and 566°C

| Stress (MPa) | Number of Bursts | Approximate Magnitude, % (Creep Stage) ^a |
|-----------------|---------------------|---|
| <u>454°C</u> | | |
| 414 | 1 | 2.7(P) |
| 434 | 1 | 3.1(P) |
| 455 | 3 | 3.2(P), 0.6(S), 0.2(S) |
| 483 | 4 | 3.7(P), 0.2(S), 0.1(S), 0.2(S), 6.6(S) |
| 483 | 1 ^b | 6.5 |
| 483 | 0 ^b | |
| 489 | 4 | 5.3(P), 1.9(S), 0.2(S), 0.3(S) |
| 496 | 7 | 1.0(P), 5.2(P), 0.5(S), 0.3(S), 0.3(S), 0.3(S), 0.3(S), 1.5(S) |
| 510 | 0 | |
| 517 | 0 | |
| <u>510°C</u> | | |
| 379 | 1 | 0.8(P) |
| 396 | 1 | 2.3(P) |
| 414 | 2 | 0.5(P), 1.1(P) |
| 434 | 1 | 3.3(P) |
| 448 | 1 | 1.0(P) |
| 455 | 1 ^b | 6.3(S) |
| 455 | 0 ^b | |
| 465 | 0 ^b | |
| 483 | 0 | |
| <u>566°C</u> | | |
| 328 | 2(?) ^c | 0.5(P), 1.0(P) |
| 345 | 2 ^b | 0.1(P), 0.2(P) |
| 345 | 1 | 0.1(P) |
| 365 | 0 | |
| 379 | 0 | |
| 396 | 0 | |
| 396 | 0 ^b | |
| 396 | 0 ^b | |
| 396 | 0 ^b | |
| 414 | 1(?) ^c | (P) ^c |
| 434 | 0 | |

^aP = primary stage; S = secondary (steady state) stage.

^bSpecimens failed prematurely.

^cStrain bursts are difficult to delineate; there are regions where the instantaneous creep rate increases instead of decreases in the primary stage.

Two of the tests failed in less than 80 hr, while the other test ruptured during a temperature excursion at 2450 hr (rupture would be predicted from Fig. 1 to occur in about 5000 hr). One of the tests that failed prematurely contained a burst of about 6% before failure. Both the premature failures had loading strains greater than 22%, whereas the 2450-hr test strained only 14% on loading (Table 2). The latter test contained a strain burst early in the test (during primary creep) of about 4% and three short bursts of less than 0.5%. Tests that contained at least one strain burst may well have had premature failures compared with those found in tests without any bursts. Our results do not permit us to conclude that such rupture lives were not premature failures.

Visual examination of the fractured specimens revealed several fracture modes as well as two types of anisotropic deformation. In many cases the surfaces appeared "fibrous" or "rumpled" with "stretcher marks" parallel to the specimen axis. Some specimens also appeared "knobby," as if one or more points on the specimen gage section were in the process of forming a neck. This "necking" was in addition to the point where the specimen necked to failure. Another indication of anisotropic behavior was the observation that specimens often drew to an elliptical cross section instead of to a circular one.

The tests at 454°C formed slight necks and in all cases exhibited the anisotropic behavior described above. Only at this temperature was there a pronounced tendency to deform to an elliptical cross section. Although at 510°C the "knobby" deformation still occurred, actually very little neck formation took place at the fracture. Note in Table 2 that the reduction of area values often nearly equaled those for total elongation, indicating little neck formation. In most cases the fractures at 454 and 510°C appeared to occur by shearing, the fracture surface making about a 45-degree angle with the specimen axis. At the lowest stresses at 510°C, however, the fracture surface made about a 90-degree angle with the specimen axis. The fracture surface contained "striations" in the direction of the shear.

The observations at 566°C resembled those at 510°C. We observed unusual behavior only in the 345-MPa (50-ksi) test that failed prematurely. In this test fracture occurred after 778.8 hr, whereas a

repeat test failed after 6003.3 hr. When the fracture surface was examined by stereomicroscopy, there appeared to be a hole on the surface. Protrusions visible inside the hole may have been dendrite tips, suggesting a defect formed during welding. While the weld itself had been radiographed before test, this specimen had not.

At 621°C, all but one of the specimens had quite flat fractures with virtually no necking. The test at 379 MPa (55 ksi), the highest stress used at 621°C, formed a slight neck and exhibited more anisotropic deformation than the other specimens did. Anisotropic deformation — both "knob" and stretcher mark" formation — decreased with decreasing stress and was absent from the lowest stress tests. Tests at 677 and 732°C showed the same behavior as at 621°C, that is, only at the highest stresses were necks and anisotropic deformation observed. The fracture surfaces of tests at 621, 677, and 732°C were "striated" like those at the lower temperatures, but they all made a 90-degree angle with the specimen axis, rather than the 45-degree angle observed for most of the tests at the three lowest test temperatures.

Radiography was used to determine whether strain bursts were accompanied by crack formation. Several specimens with strain bursts of up to 5% were examined. This technique can detect cracks or voids of 0.08–0.13 mm (0.003–0.005 in.), but we observed none.

Selected specimens were examined metallographically. At all temperatures, cracks were detected in grain boundaries back from the fracture surface (Figs. 10–13). For all stresses at 454°C and for the highest stresses at 510 and 566°C, only a few grain-boundary cracks were detected, and they were widely scattered on the specimen gage section (Fig. 10). The number of grain-boundary cracks increased with a decrease in the creep stress at 510 and 566°C. For the lower-stress tests at 510 and 566°C, we observed flat fractures with essentially no necking and little deformation near the fracture surface (Figs. 11 and 12). The fractures of both these specimens appeared to be intergranular. Part of the fracture surface on the 345-MPa-test specimen at 566°C appeared oxidized, suggesting that it fractured earlier in the test.

Fractured specimens at 621, 677, and 732°C all showed apparent transgranular failures at the highest stresses. As the stress was

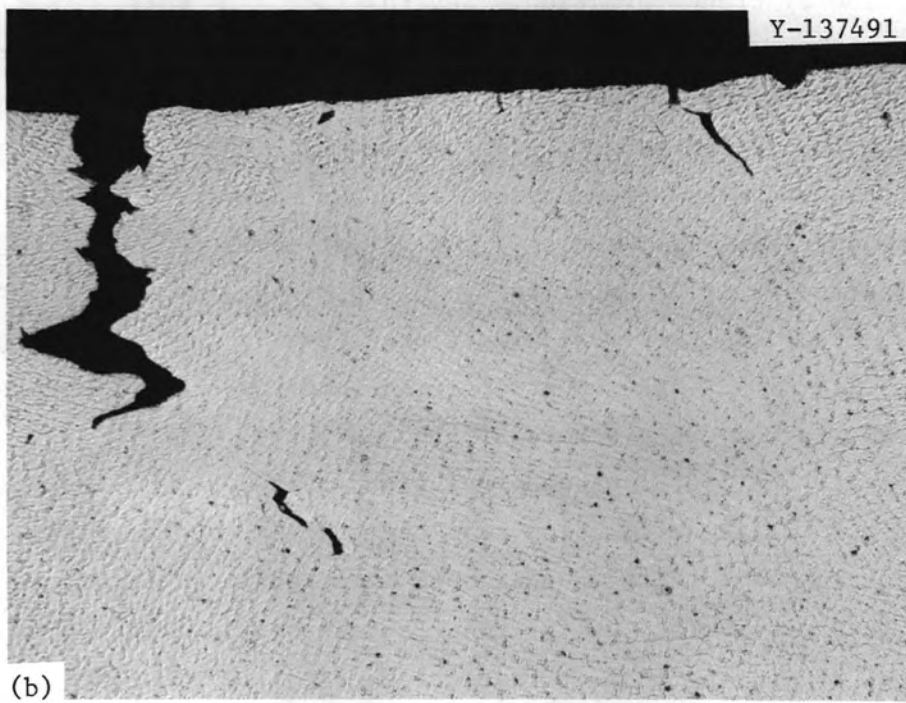


Fig. 10. Scattered Grain Boundary Cracks on Specimen Tested at 396 MPa at 566°C. (a) Unetched 50×. (b) Etched with 5:1 HCl:HNO₃. 100×.

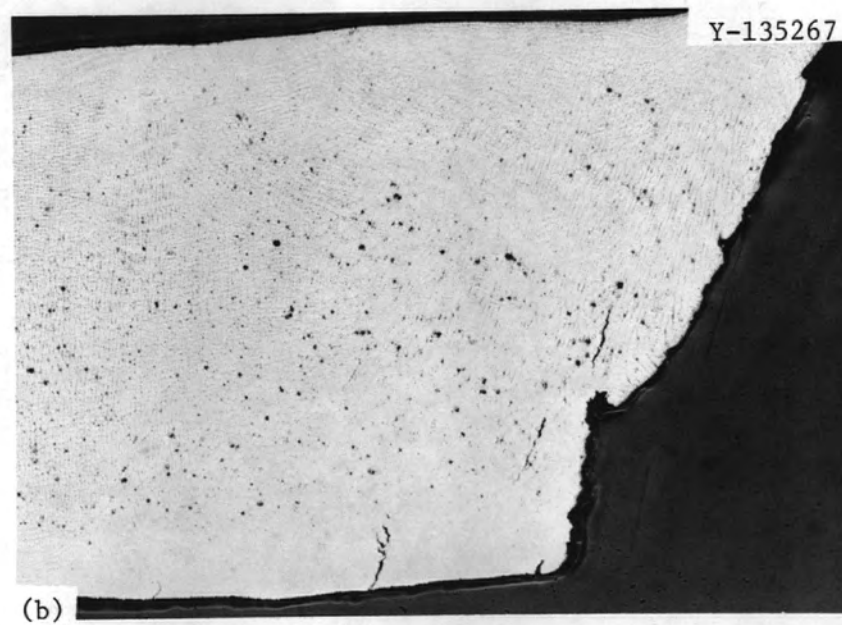
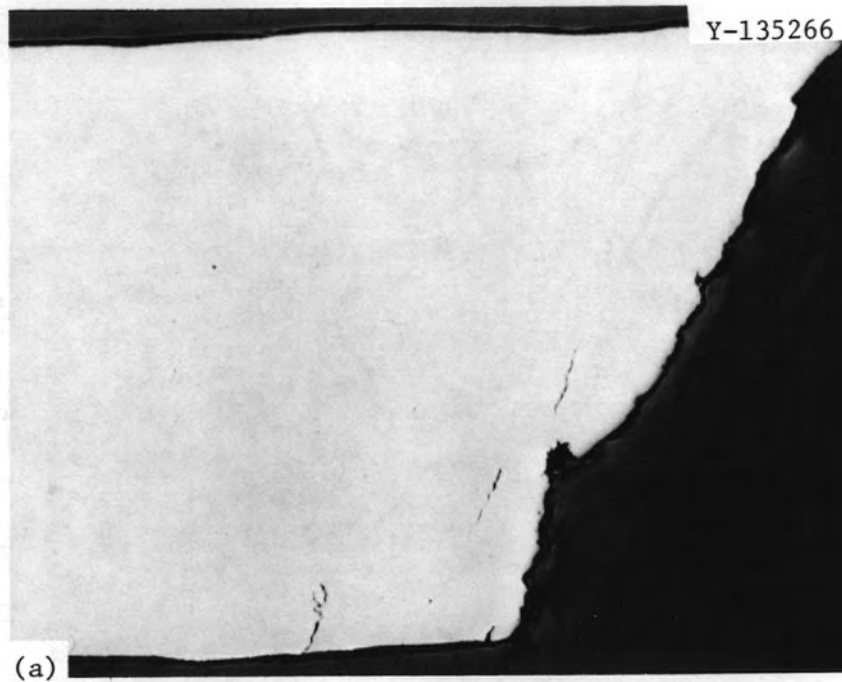


Fig. 11. Grain Boundary Cracks on Specimen Tested at 413 MPa at 510°C. (a) Unetched. (b) Etched with 5:1 HCl:HNO₃. 50×.

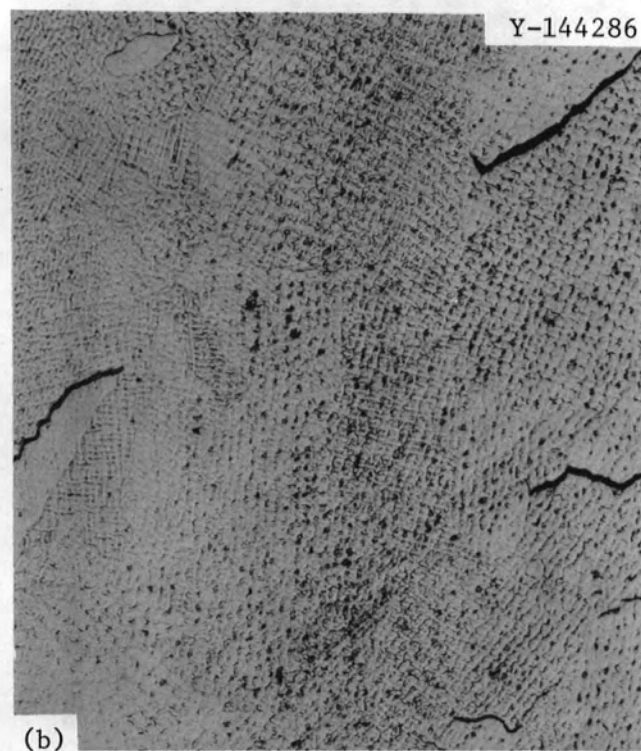
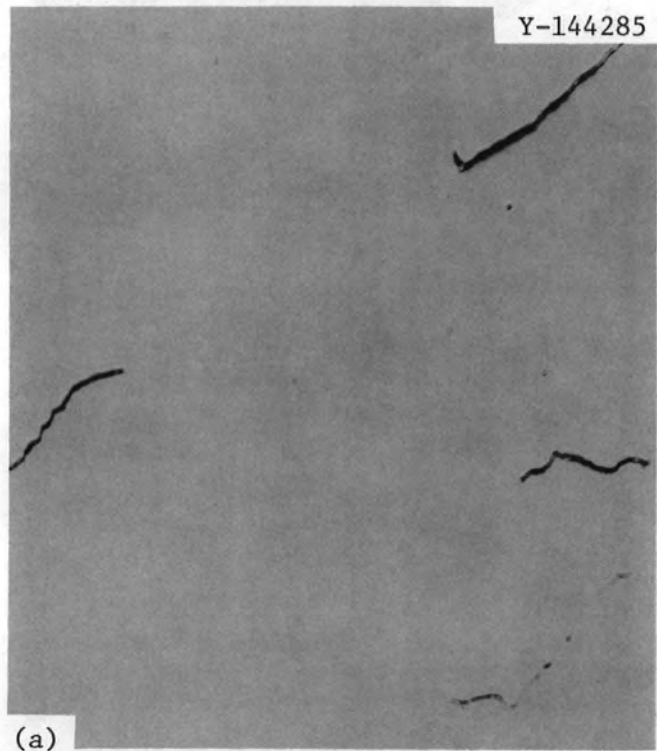


Fig. 12. Grain Boundary Cracks on Specimen Tested at 345 MPa at 566°C. (a) Unetched. (b) Etched with 5:1 HCl:HNO₃.

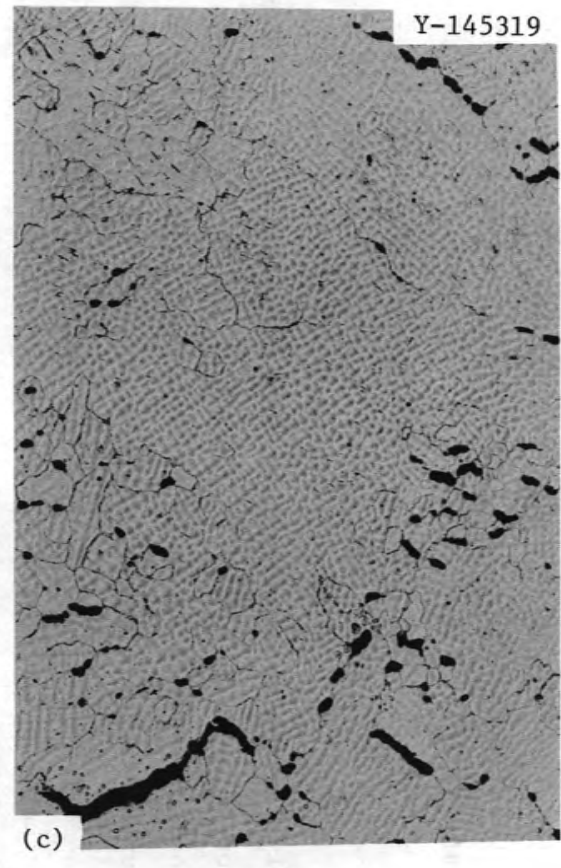
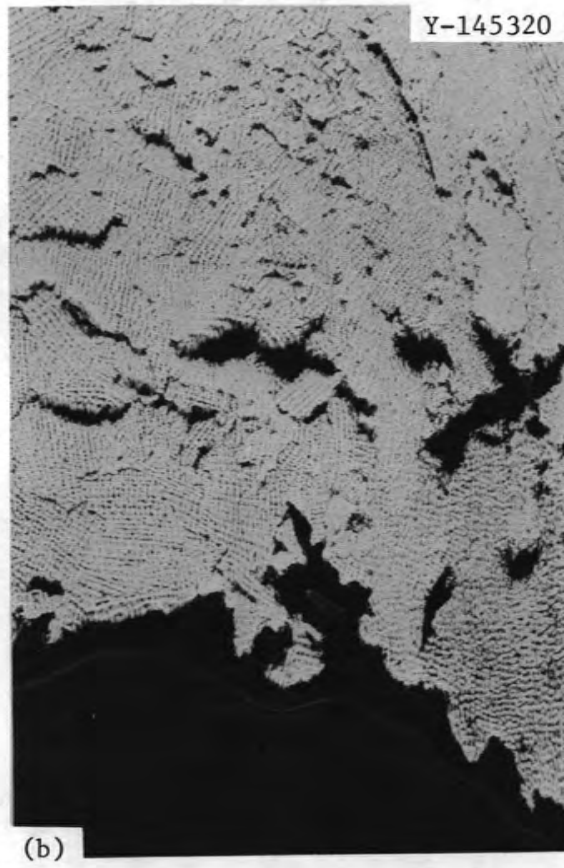
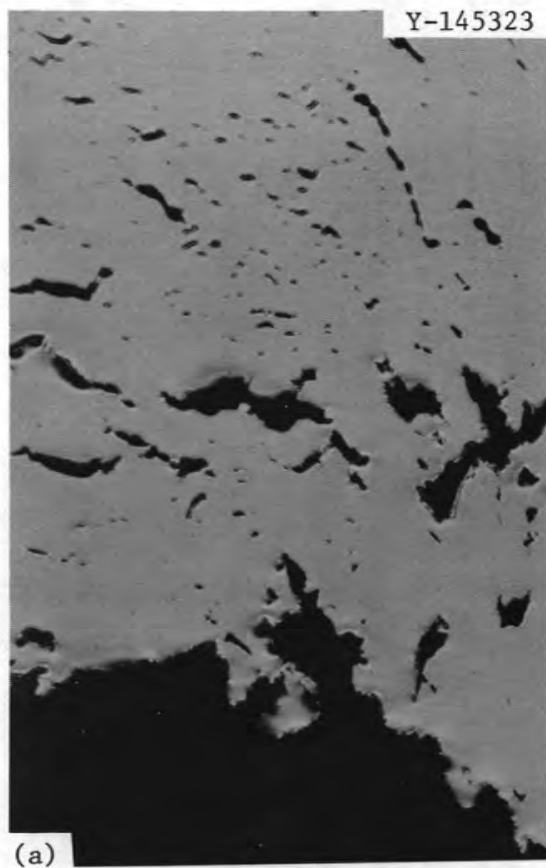


Fig. 13. Example of Grain Boundary Cracks and Cavities in a Specimen Tested at 83 MPa at 732°C. (a) and (b) are near fracture surface, 50×. (c) In gage section back from fracture surface, 100×. (b) and (c) were etched with 5:1 HCl:HNO₃.

lowered and the temperature raised; the failures became more intergranular and grain boundary cracking in the specimen gage length (back from the fracture surface) increased (Fig. 13).

DISCUSSION

The only available creep-rupture data for comparison are those obtained by Huntington Alloys⁴ at 538, 649, 760, 871, and 982°C. These data consist of only two or three tests at each temperature, enough data to determine rupture and minimum-creep-rate curves. Our data at 566°C fall on the line given by Huntington Alloys at 538°C. At the higher temperatures, our data bracket the Huntington Alloys data: our 621 and 677°C data fall on either side of the 649°C data, and the 732°C data fall as expected relative to the 760°C data.

When we compared our tensile data with Huntington Alloys data,² we found the Huntington Alloys material somewhat stronger at all test temperatures. We concluded that this difference arose from the fact that the material tested by Huntington Alloys was in an as-welded condition, whereas our material had been tempered 1 hr at 732°C after welding. If the postweld treatment created the tensile property differences, it did not appear to affect the creep properties. This assumes, however, that Huntington Alloys used the same weld metal for both the tensile and the creep tests, an assumption we were unable to verify.

The specimens tested at 510 and 566°C were taken from welds made with about 7 weld passes on 13-mm-thick plates, while specimens tested at 454, 621, 677, and 732°C were from welds made with more than 40 weld passes on 19-mm-thick plates. From the tensile studies² we concluded that while weldment size affects yield strength slightly at elevated temperatures, it affects ultimate tensile strength even less. We further conclude that the only expected difference in the two weldments should be due to the dilution of the weld metal by the base metal. Iron from the 2 1/4 Cr-1 Mo steel plates was found to be the only major diluent.² The dilution of the large weldment was confined close to the interface between the weld metal and the base metal, while the small weldment contained approximately 10% iron throughout. The tensile studies thus

indicated no large dilution effect.² Payne³ indicated that dilution by iron should increase the strength, but our results did not indicate strengthening.

Although most of the tests at 566°C were made on specimens taken from the 13-mm-thick plates, several were also made on specimens from the larger weldment. Again, no conclusive difference was noted, though the number of tests involved was small (Table 2). For comparison two specimens from the large weld tested at 396 MPa failed much sooner than did one from the smaller weldment. Both were judged to fail prematurely. On the other hand, test data from a specimen taken from the large weldment and tested at 345 MPa fell on the creep-rupture and minimum-creep-rate curves (Figs. 1 and 2) plotted from test data from specimens taken from the small weldments. On the other hand, a specimen from the small weldment failed prematurely at 345 MPa. Thus, these few tests suggest no dilution effects or other differences that could be attributed to difference in the size of the weldments from which the specimens were taken.

The creep-curve shapes at the low temperatures indicate logarithmic creep behavior with a strain-time relation of the type

$$\epsilon = \alpha \log t + c , \quad (3)$$

where ϵ is the creep strain, t is the time, and α and c are constants that are independent of time. Such a relation has been found⁸ to apply to several metals and alloys at low homologous temperatures, that is, at low T/T_m , where T is the test temperature and T_m the melting temperature in K. Garofalo⁸ stated that Eq. (3) applied for T/T_m of 0.05–0.3. For ERNiCr-3, T_m is about 1700 K and T/T_m is 0.27, 0.30, and 0.33 for 454, 510, and 566°C, respectively, near the upper limit of the region where Garofalo indicated Eq. (3) applies.

Logarithmic creep implies a creep curve with a constantly decreasing creep rate. Obviously, that was not strictly true for the tests in this study, since all the tests were judged to reach a steady state. However, the difficulty in determining a steady state for a creep test that has not gone into tertiary creep is well known.⁹ Several of the low-stress

tests at 454°C fall into this category. Similarly, at the low stresses at 510 and 566°C, limited tertiary creep makes the minimum creep rate uncertain.

To determine whether Eq. (3) applied, we plotted the strain against $\log t$ for the early portion of the low-stress tests at 454, 510, and 566°C (Figs. 14 and 15). The two low-stress tests (413 and 434 MPa) at 454°C indicated logarithmic creep (Fig. 14). The curve for the 413-MPa test appeared linear to 2500 hr, while the curve for the 434-MPa test was linear to about 2000 hr, then showed an upward curvature. Such upward curvature was obvious at 455 MPa at 454°C (Fig. 15). Plots of the low-stress tests at 510 and 566°C displayed downward curvature (Fig. 15).

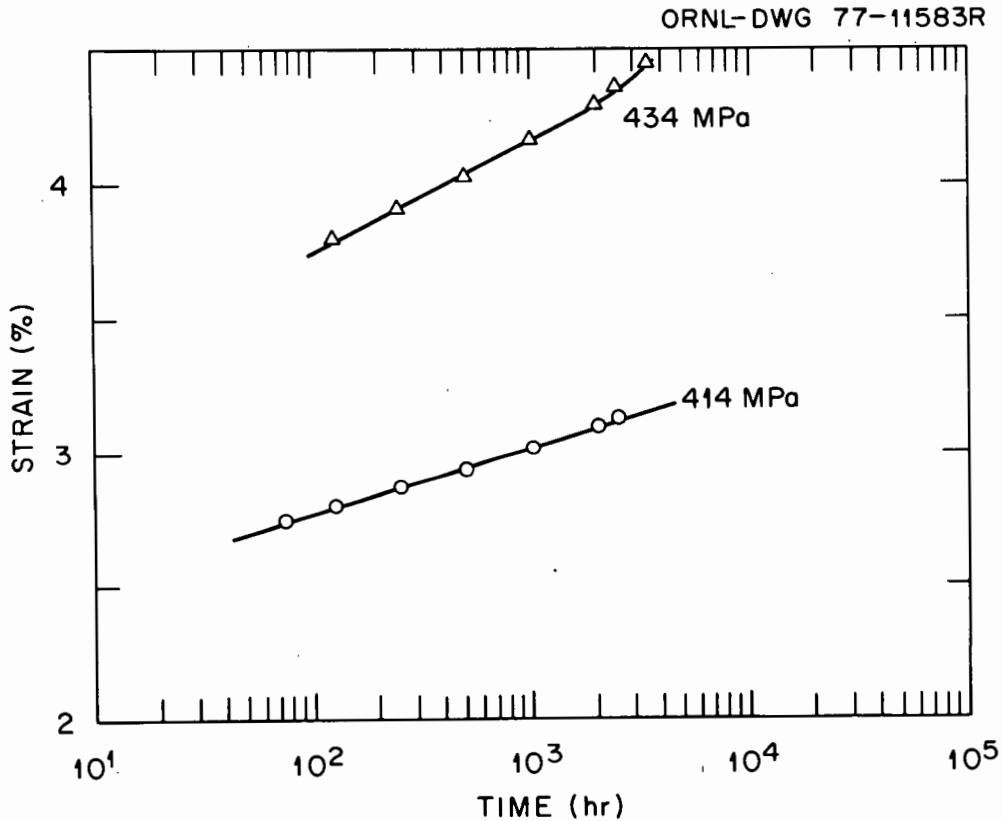


Fig. 14. Semi-Logarithmic Plot of Creep Data for ERNiCr-3 Weld Metal Tested at 413 and 434 MPa at 454°C.

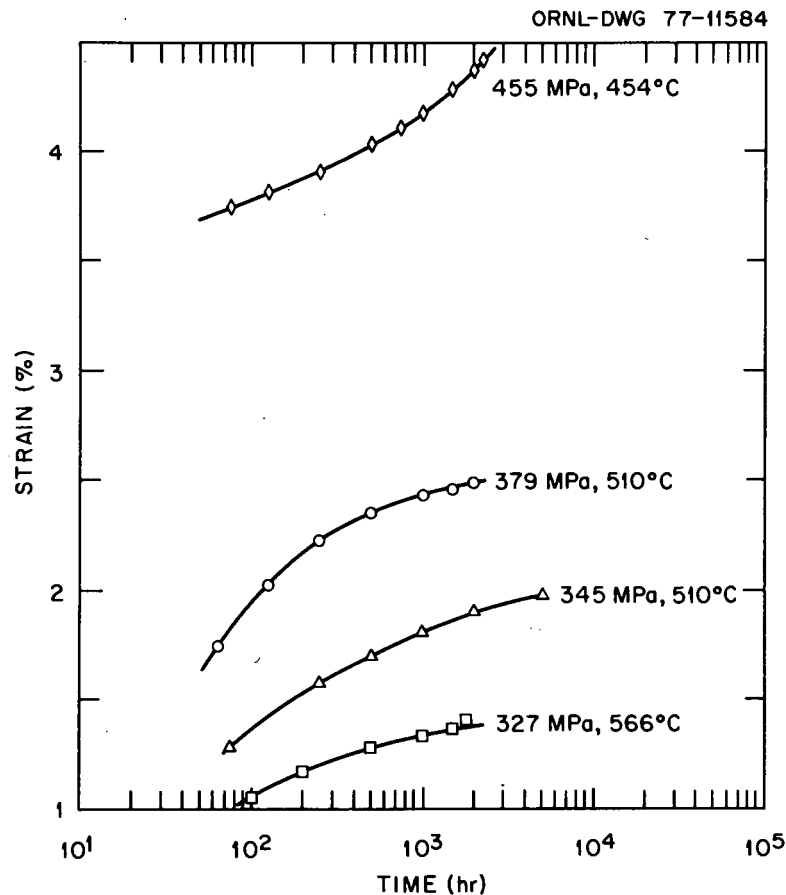


Fig. 15. Semi-Logarithmic Plot of Creep Data for ERNiCr-3 Weld Metal Tested at 455 MPa at 454°C, 345 and 379 MPa at 510°C, and 327 MPa at 566°C.

While logarithmic creep is confined to a low homologous temperature range, it is also confined to low strains. According to Garofalo,⁸ it occurs to strains of about 2×10^{-3} . The total "creep" strains for the two tests at 454°C were considerably larger. However, early in both these tests a strain burst of about 3% took place. The strains used in Fig. 14 were creep strains measured after the strain bursts had occurred. When the strains caused by the strain bursts were ignored, strains of up to about 5×10^{-3} were found for the two low-stress tests at 454°C.

Logarithmic creep, therefore, apparently occurs at low stresses at 454°C. Obviously, more tests at lower stresses are required to verify this behavior and determine the effect of stress on the constants in Eq. (3). Because the tests at 510 and 566°C as well as those at the

higher stresses at 454°C do not follow Eq. (3), some other creep law must apply. The test at 455 MPa at 454°C seems to fit a parabolic law of the type

$$\dot{\epsilon} = \beta t^m + \dot{\epsilon}_s t, \quad (4)$$

where β and m are constants and $\dot{\epsilon}_s$ is the steady-state creep rate. However, this equation did not fit the low-stress tests at 510 and 566°C.

Numerous other empirical creep laws have been used to fit strain-time data at elevated temperatures and for large deformations. To determine such a law for ERNiCr-3 was beyond the scope of the present study. That subject will be addressed in later work. In addition to the different types of behavior noted at the different test temperatures, the development of a creep law will be further complicated by the strain burst phenomenon.

We cannot readily explain the strain burst phenomenon. Some obvious possibilities include: test technique, neck formation, and void or crack formation. Another possibility is gross change in microstructure (e.g., recrystallization), but no such changes were detected.

If the test technique were the cause, we would expect the bursts to occur at temperatures other than 454, 510, and 566°C. As we stated earlier, no strain bursts occurred at 621, 677, and 732°C. The test procedures used in this study have been used at these temperatures in other test programs and for a large number of materials, but no strain bursts resulted. Grip slippage is the most obvious test procedure malfunction that could produce strain bursts. However, this would be obvious when the total elongation determined from measurements on a fractured specimen is compared to that measured during the creep test.

It is difficult to visualize how neck formation and void or crack formation could ever lead to an instantaneous elongation of greater than 5% without fracture. That is, such a large decrease in cross-sectional area should immediately lead to a large increase in stress and instantaneous fracture. (Later in this section we will discuss how the premature failures at 454, 510, and 566°C may be related to instability.) Inspection of unfractured specimens after a large strain burst revealed no necking. Similarly radiography of fractured and unfractured specimens after a strain burst detected no cracks or voids.

Once we eliminate the possible causes we cited above for the strain bursts our observations suggest that deformation is somehow prevented until stress builds up to a critical level. Then the built-up stress is unlocked, and the specimen suddenly strains. On an atomic level we visualize dislocation pileups at some barrier within a given grain. These piled-up dislocations would be in addition to a distribution of mobile dislocations that allows for "normal creep."

Eventually, the stress buildup on an isolated pileup forces the lead dislocation through the barrier. Once the lead dislocation breaks through the barrier, the dislocations behind it are released in a "dislocation avalanche." The avalanche then triggers the release of pileups in the same grain and in neighboring grains. The net result is a "deformation band" that moves up and down the gage section in a manner similar to the movement of a Luders band along a gage section. A similar result may occur if certain locked dislocation sources are triggered, and, in turn trigger neighboring sources in the same grain and neighboring grains.

In our tensile studies on ERNiCr-3, we observed pronounced peaks in the flow stress for tests made at slow strain rates (3×10^{-6} /s), but not for tests at a higher strain rate (3×10^{-4} /s). For the low strain rate the yield strength peak occurred over the temperature range 454–700°C, while the ultimate tensile strength peak occurred between 400 and 600°C. A yield strength maximum occurred around 550°C, while the ultimate tensile strength had a local maximum near 500°C. We concluded that these effects were caused by short-range order.² (Interestingly, this effect was a maximum in the temperature regime in which the strain bursts were observed.)

We previously reviewed² the evidence for short-range order — often referred to as the "K-state" — in nickel-chromium alloys¹⁰⁻¹³ and more complicated alloys with a nickel-chromium base, including Inconel 600,¹³ which is somewhat similar in chemical composition to ERNiCr-3. Most of these studies involved measurements of electrical resistivity as a function of temperature. Instead of increasing continuously with temperature as expected, resistivity only increases to 450–500°C then goes through a local minimum between 500–700°C. Williams¹⁴ observed similar behavior in ERNiCr-3 weld metal.

Fisher¹⁵ first showed that the strength of an alloy with short-range order must be greater than one without such order. When a dislocation moves through an ordered region, it destroys order. Because more energy is required to break the order bonds, it is more difficult to move a dislocation through the ordered lattice. However, once the first dislocation destroys the order, subsequent dislocations can move across that disordered slip plane at a reduced stress.

When the amount of order in a given alloy increases — for example, by prolonged annealing below T_c , the critical temperature to form long-range order — the energy required to form the disordered slip plane by moving a dislocation through the ordered region increases. Eventually a single dislocation cannot move through the ordered zone.¹⁶ Deformation then proceeds by the movement of superdislocations that consist of paired dislocations connected by a segment of anti-phase boundary. The second dislocation restores the order bonds broken by the passage of the lead dislocation across the slip plane. When the super-dislocation passes through the ordered zone, the order bonds remain intact.

Using the Fisher mechanism¹⁵ we explained² our tensile observations in terms of short-range order. For the high strain-rate tests the first dislocation that moves through a short-range order zone destroys order bonds on that slip plane, and consequently, later dislocations require less energy to move across the same slip plane. At the low strain rates at which the peak in flow stress is observed, dislocation velocity is much reduced. In this case the order destroyed by the initial dislocation can be restored by diffusion before another dislocation can move across that slip plane. Hence, as it passes through, each dislocation must break the same order bonds broken by dislocations that passed through the region earlier.

Because the temperature range in which the strain bursts appeared was similar to that in which the increased flow stress was noted for the low strain-rate tensile tests² and the range where the anomalous resistivity behavior was observed,¹⁴ we can speculate that the strain bursts are related to short-range order. We can envision an alloy with short-range order formed when the material was cooled after the postweld temper at 732°C and when the specimen was heated to the creep-test temperature. If we assume that dislocations are moved through these order

zones with great difficulty (i.e., the Fisher mechanism),¹⁵ we can visualize the formation of dislocation pileups at regions of short-range order. As a pileup builds, the stress on the lead dislocation increases and it moves through the ordered zone. The pileup of dislocations that follow in its wake will move more easily as the number of order bonds on the slip bands are reduced by the initial dislocation. Once the lead dislocation breaks through the order zone, the other dislocations in the pileup immediately follow. This avalanche of moving dislocations then triggers the release of pileups in the same grain and in neighboring grains. As more and more grains are triggered, an inhomogeneous deformation wave moves up and down the specimen gage length in a Luder's band type of deformation mode. In other words, a strain burst.

Based on the electrical resistance measurements¹⁴ and the tensile studies² that definitely indicate order formation, the proposed mechanism appears reasonable. However, the possibility exists that the behavior is peculiar to cast structures, as distinguished from wrought structures. This possibility was raised by some studies by Sikka¹⁷ on type 316 stainless steel. Although only a limited amount of data have been obtained on the cast material, Sikka noted strain bursts in several tests but has never seen similar behavior in much more extensive studies on wrought type 316 stainless steel.

The microstructures of the cast and wrought ERNiCr-3 show significant differences (Fig. 16). The fine dendritic solidification structure with its accompanying chemical inhomogeneities within a given grain could well give rise to differences in mechanical property behavior. Although the proposed mechanism would still apply — that is, that dislocation pileups are triggered and give rise to dislocation avalanches and a Luders-type deformation — the pileups could result from the fine dendritic structure within the grains. We could also hypothesize that the cast structure in conjunction with short-range order formation gives rise to the much more extensive activity observed in ERNiCr-3 weld metal.

With only a few exceptions all specimens that displayed the strain burst phenomenon had bursts during the primary creep stage (Table 6), while the ones that did not failed prematurely. At 454, 510, and 566°C, all loading strains exceeded 5% and most exceeded 10% (Table 2). These

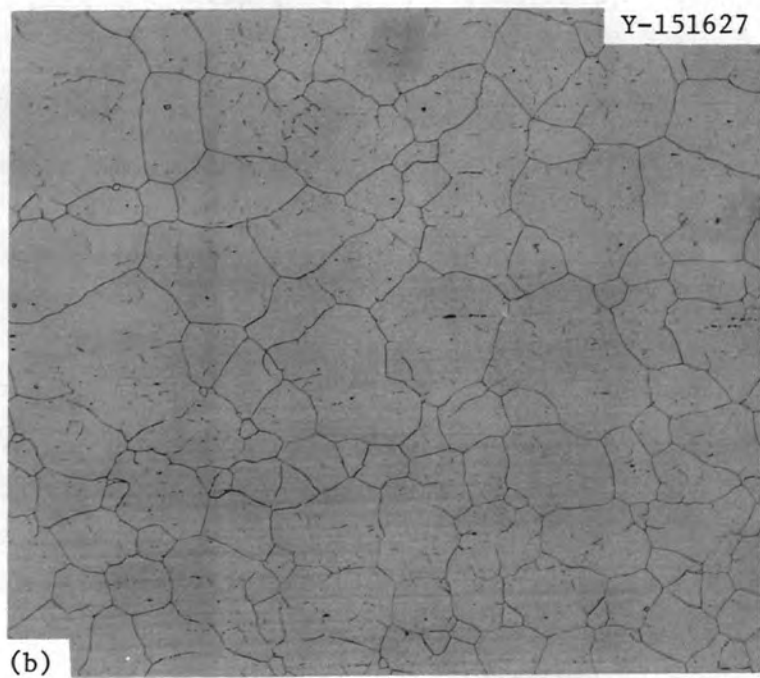
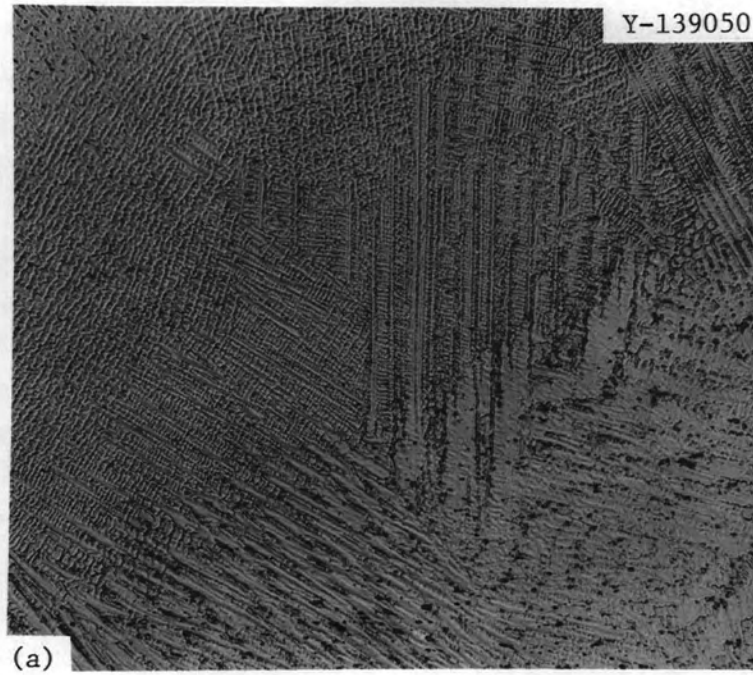


Fig. 16. The Microstructures of (a) Weld Metal (Cast) and (b) Wrought ERNiCr-3. 100 \times .

results indicate that dislocation pileups could form during loading, and that a strain burst during the primary creep stage subsequently relieved such pileups. The three specimens that did not have strain bursts in the primary stage had significantly greater loading strains than those that did, indicating that strain bursts probably occurred during loading in this case.

Virtually all tests at 454°C showed extensive strain burst activity. Although strain bursts early in the primary stage presumably relieved the pileups that occurred during loading, additional pileups had to form, leading to strain bursts during the secondary stage. In most cases these strain bursts in the steady-state stage were much smaller than those in the primary stage (Table 6).

The magnitude of the strain bursts during the primary stage for the four lowest stress tests (414, 434, 455, and 483 MPa) at 454°C decreased slightly with decreasing stress. Intuitively, we expect this, since the lower the stress is, the less is the extent of pileup formation expected during the loading process. The tests at 455 and 483 MPa also had strain bursts during the steady-state stage, whereas those at 414 and 434 MPa did not. However, the latter two tests were discontinued before rupture. Thus although the pileups formed during loading are released by the strain burst during the primary creep stage, pileups again form. The higher the creep stress, the more quickly pileups form and are released by a strain burst. From this we might expect that if the tests at 414 and 434 MPa had been continued, strain bursts would have occurred, since at the lower stress the dislocation at the head of the pileup simply takes longer to force itself through the barrier than at higher stresses. Only more long-term low-stress tests will verify this.

At 510 and 566°C all but one of the specimens that displayed strain bursts had the bursts during primary creep; the exception was a premature failure discussed above. The tests with strain bursts were the low-stress tests. These results seem to indicate that at the highest stresses it is possible to force dislocations continuously through the barrier — an ordered region or regions associated with the dendritic cast structure. As the stress is lowered, a stress is reached where the dislocations cannot be continuously forced through the barrier and they pile up, followed eventually by a strain burst.

The fact that the strain burst activity decreases with increasing temperature may be attributed to one of two processes, depending on the cause of the dislocation pileups: (1) The amount of order formed decreases with increasing temperature because of thermal fluctuations, (2) The inhomogeneities of the cast structure have less effect on the material because at elevated temperatures, diffusion produces a leveling of those inhomogeneities.

From the above discussion, we should be able to qualitatively predict the strain burst behavior at stresses lower than those used in this study. As the stress is lowered, the magnitude of the strain burst in the primary stage should continue to decrease; that is, as the loading strain decreases, the extent of the initial pileups should decrease. Eventually, a stress should be reached at which strain bursts no longer occur during the primary stage. However, strain bursts should continue to occur during the steady-state stage. This follows because the stress will be too small to move dislocations continuously through the barriers.

The two postulated dislocation barriers give rise to different predictions concerning continued strain burst activity for low-stress long-time tests. In such tests, the specimens would be subjected to the test temperatures for a long period. If order formation is assumed to be completed over a long time, then the continued order formation during test could lead to more ordered regions, which would result in continued (or perhaps increased) strain burst activity. On the other hand, if the cast structure is responsible for preventing dislocation movement, the prolonged exposure at temperature could lead to homogenization, which would, in turn, lead to a decrease in strain burst activity. Hence, long-time low-stress tests or tests after aging should result in reduced strain burst activity if the cast structure facilitates strain bursts but in heightened activity if an ordered structure induces the strain bursts. Tests at the highest temperature, 566°C, should allow us to distinguish such behavior. At the lower temperatures, 454 and 510°C, strain burst activity will probably continue longer, because if the cast structure is responsible for the strain bursts, at these temperatures diffusion will only slowly eliminate the inhomogeneous structure.

In the future we intend to compare the creep behavior of wrought material to that of weld metal. This study, along with transmission electron microscopy studies and low-stress tests on weld metal, should help to determine the cause of the strain bursts. The effect of thermal aging will also be investigated. If an ordered structure forms at 454–566°C, then the strength of the weld metal would be expected to increase, as observed in the tensile studies.²

Although no extensive literature search was undertaken, two reports of related observations of instantaneous elongation – "periodic strain"¹⁸ or "strain bursts"¹⁹ – were found. Lubahn noted that 61ST – an aluminum alloy with approximately 0.25 wt % Cu, 0.6 wt % Si, 1.0 wt % Mg, and 0.25 wt % Cr – "tested in creep at room temperature several months after commercial aging exhibited smooth strain-time curves." However, when tested "... within a few hours after the commercial aging treatment [it] exhibited sudden periodic extensions superimposed on a smooth strain-time curve." Lubahn's "periodic extensions" were much smaller – less than 0.1% – than those observed in ERNiCr-3. Lubahn recorded more than ten jumps in a ten-hour test, instead of the few large jumps noted for ERNiCr-3.

Lubahn pointed out that Andrade²⁰ noted a similar phenomenon for copper tested at room temperature. Andrade's description is interesting: "A peculiarity of copper wire was that it showed sudden slips at irregular intervals, which perhaps may be called 'copper quakes' as being analogous to the geological slipping supposed to result in earthquakes." Again these "copper quakes" were small.

Lubahn¹⁸ discovered a second effect in 61ST that "is aging rapidly during deformation." He found "... that a large plastic extension occurred upon application of the load, after which the material did not elongate further. Furthermore, successive additions of small load increments never caused gradual straining. After each load increment, either sudden plastic extension occurred or the specimen remained elastic." Lubahn attributed both the "periodic extension" and the "sudden plastic extensions" to the fact that the "metal is aging while it is being plastically deformed."

Chalco¹⁹ observed a behavior similar to Lubahn's "sudden plastic extensions," the second effect cited earlier. In two low-carbon 2 1/4 Cr-1 Mo steels, Chalco found that "... very often an increment of stress was accompanied by a strain burst... ." The increment of stress required was about 14 MPa (2 ksi) in a test often already loaded to 345 MPa (50 ksi). Chalco noted extensions of up to 1%. He labeled his observation a "strain burst," although he did not explain it. We adopted this description although the strain bursts exhibited by ERNiCr-3 differ from both the second type found by Lubahn and those found by Chalco. They more nearly resemble Lubahn's "periodic extension" and Andrade's "copper quakes." We tried to produce a strain burst by adding small increments of load to a specimen creeping in the steady-state stage at 510°C, but no strain burst occurred.

Lubahn's observation that the "sudden periodic extensions occurred when the alloy is aging rapidly during deformation," applies to the one explanation advanced for the behavior of ERNiCr-3 weld metal. During test at the temperatures at which strain bursts occurred, short-range order was forming.

Since the premature failures occurred at 454, 510, and 566°C — the same temperatures as the strain bursts — a connection was naturally sought. A premature failure may be considered a "strain burst to infinity" — strain bursts that continue beyond a limited strain jump. The microstructure of the welds may ultimately help explain the connection between strain bursts and premature failures.

The as-welded ERNiCr-3 was previously shown to contain very small defects scattered through the microstructure,² defects of a size that radiography could not detect. These defects were always found in grain boundaries and often appeared to be grain boundary cracks (Fig. 17). The tensile failures occurred transgranularly. However, we found no direct evidence to relate the cracks to the grain boundary defects observed on the as-welded material, although we suspected that they were connected.

As the temperature was increased and the creep stress decreased, grain boundary separation became more important to the fracture process. On the other hand, at all stresses at 454°C and at all but the lower stresses

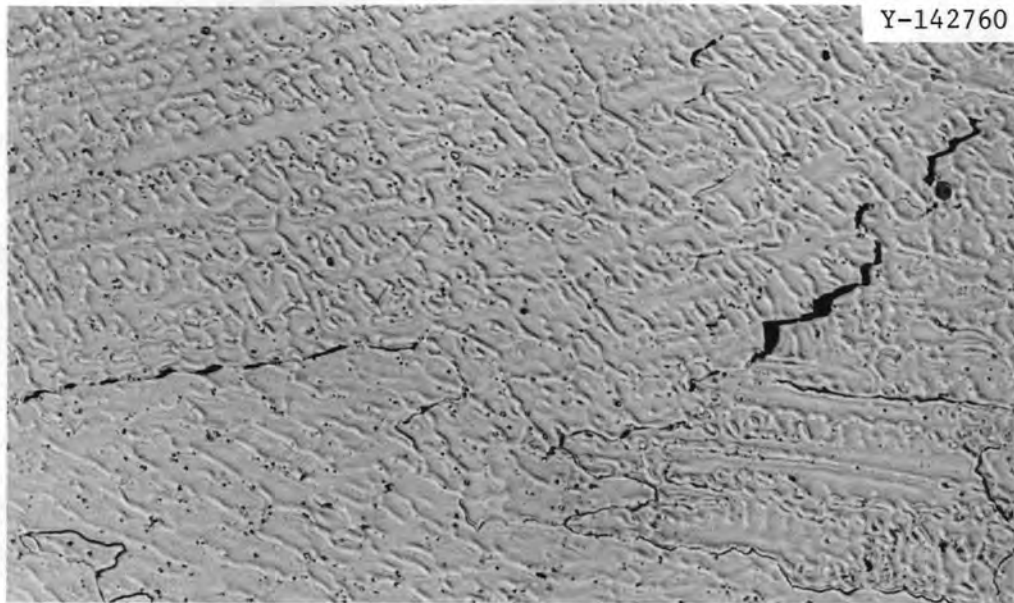


Fig. 17. Example of Scattered Cracks or Voids That Were Observed in As-Welded ERNiCr-3. Etched with 5:1 HCl:HNO₃. 200×.

at 510 and 566°C, the failures were transgranular. Nevertheless, as was true for the tensile tests, there were again scattered instances of grain boundary separation. And again, we must logically suspect a connection between these grain boundary cracks and those seen in the as-welded microstructure.

The "knobby" deformation was previously related to the microstructure of the weld.² Similarly, in creep specimens metallographically examined (Fig. 18), knobs often appeared on the surface near the position where several grain boundaries met [Fig. 18(a)]. In other cases the knob resulted from grain boundary cracks in material adjacent to the external surface.

The connection between strain bursts and premature failures may well lie in the origin of the knobby deformations. If during a large strain burst, an instability — a knob, which is really the start of a neck — develops, it could lead to failure. This is especially true if that instability results from a grain boundary crack such as that shown in Fig. 18(b). Neck formation is favored by high strain rates and low temperatures and the strain rates during a strain burst would appear to be quite large. Hence, if a cavity is present in conjunction with the

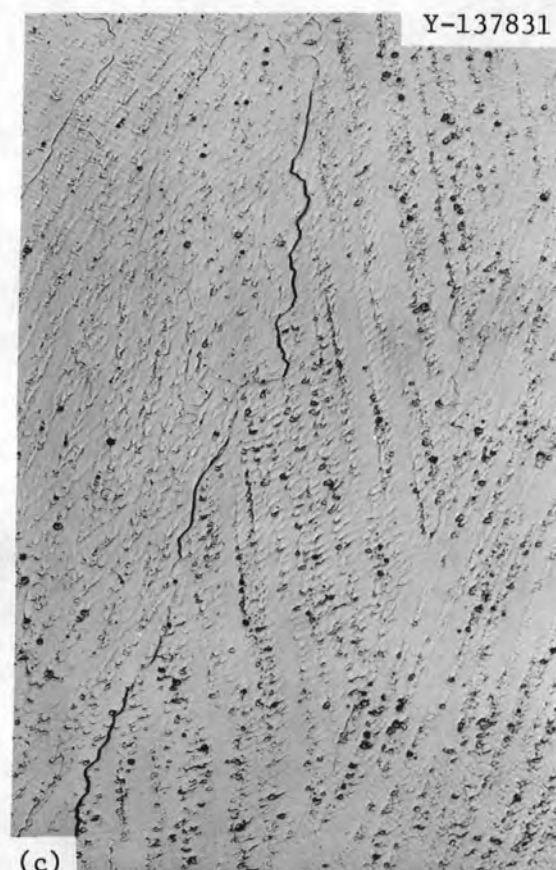
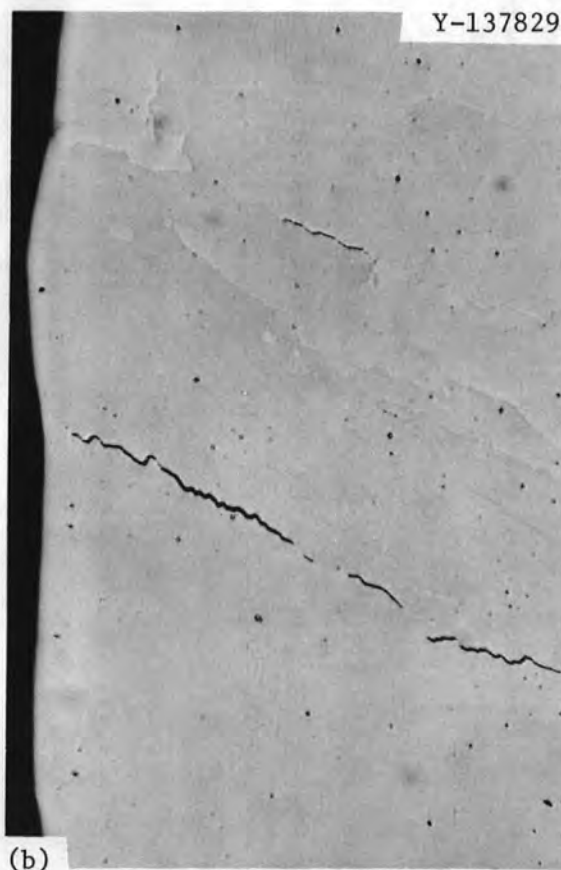
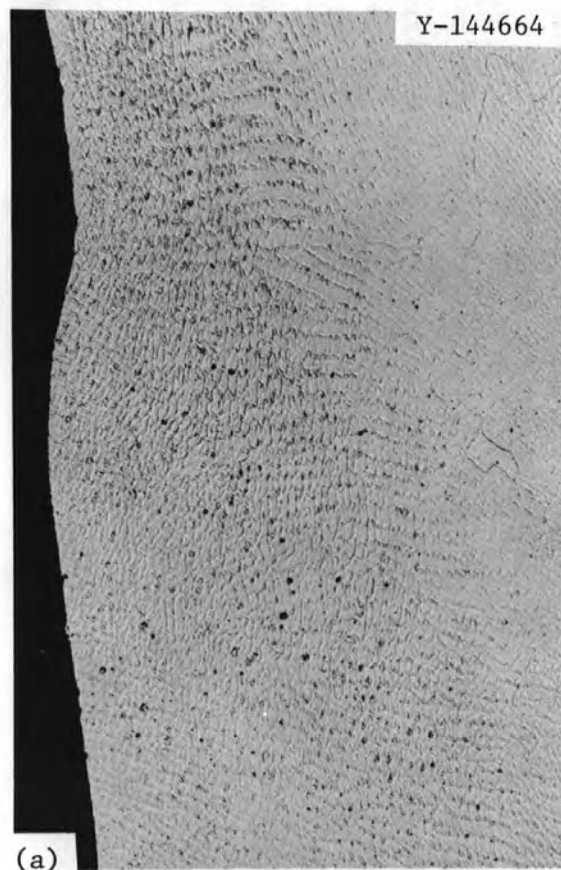


Fig. 18. Photomicrographs That Demonstrate the Cause of "Knobby" Deformation During Creep. (a) Adjacent to position where several grains meet. 100 \times . (b) Adjacent to grain boundary cracks. 50 \times . (c) Enlarged view of crack in (b). 100 \times . (a) and (c) were etched with 5:1 HCl:HNO₃.

neck (knob), deformation can then proceed to failure, turning the creep test into a tensile test. At 621, 677, and 732°C, there were knobby deformations only for a few of the higher stresses and no premature failures.

SUMMARY AND CONCLUSIONS

Creep-rupture tests were made on ERNiCr-3 (Inconel 82) weld metal over the range 454–732°C. Tests were made on weld metal specimens taken from weldments made with the automatic gas tungsten-arc process with cold-wire filler additions. The following summarizes the results and conclusions:

1. Metallography revealed scattered grain boundary "cracks" or "voids," which radiography could not detect.

2. Creep behavior fell into two temperature regimes, which respectively consisted of tests at 454, 510, and 566°C and tests at 621, 677, and 732°C. Although the 621°C-test results generally resembled those at 677 and 732°C, their characteristics often fell between those of the low- and high-temperature regimes.

3. The creep-rupture curves in the low-temperature regime were quite flat — especially at high stresses — and were characterized by a change in slope. Similar behavior was noted for logarithmic plots of stress against minimum creep rate. Stress exponents from the latter plots were on the order of 25–30 for the low-stress tests for the low-temperature regime, as opposed to values of 8–10 for the high-temperature tests.

4. Creep curve shapes differed for the two temperature regimes. At the low temperatures, creep curves were characterized by a high initial creep rate followed by a rapid transient to the steady state, and essentially no tertiary creep. Creep curves for tests in the high-temperature regime displayed a lower initial creep rate, less steady-state creep, and a longer period of tertiary creep.

5. For certain tests at 454, 510, and 566°C, the creep curves exhibited strain "jumps" termed "instantaneous elongation" or "strain bursts." Such strain bursts were observed during primary creep and/or during the steady-state stage. The percentage of tests that displayed such strain bursts increased with decreasing temperature: that is, 40% of tests at 566°C, 67% at 510°C, and 73% at 454°C exhibited them. No strain bursts were observed above 566°C.

6. Several tests at 454, 510, and 566°C ruptured prematurely, that is, the tests did not obey the rupture curves established by the majority of tests. Evidence suggested that the premature failures were related to both the strain burst phenomenon and the scattered holes that were observed by optical microscopy in the as-welded alloy.

7. We postulate that the strain burst phenomenon is connected with the formation of dislocation pileups within the matrix. The localized release of a pileup triggers neighboring pileups and gives rise to the propagation of a Luder's deformation band along the gage length. The pileups may either result from the formation of short-range order in the alloy or be peculiar to the ERNiCr-3 cast structure, as opposed to a wrought structure. A combination of these two factors may also help create pileups and strain bursts.

ACKNOWLEDGMENTS

We wish to acknowledge several people who were instrumental in completing this work: J. L. Griffith conducted the creep tests; C. W. Houck carried out the metallography; D. P. Edmonds, V. K. Sikka, C. R. Brinkman, and G. M. Slaughter reviewed the manuscript; N. W. Richards edited the manuscript; and K. A. Witherspoon prepared the final version of the report.

REFERENCES

1. J. F. King, M. D. Sullivan, and G. M. Slaughter, "Development of an Improved Stainless Steel to Ferritic Steel Transition Joint," *Weld. J. (Miami)* 56(11): 354s-358s (1977).
2. R. L. Klueh and J. F. King, *Elevated-Temperature Tensile Properties of ERNiCr-3 Weld Metal*, ORNL-5354 (December 1977).
3. B. E. Payne, "Nickel-Base Welding Consumables for Dissimilar Metal Welding Applications," *Met. Constr. Br. Weld. J.* 1(12s): 79-87 (1969).
4. Private communication, Huntington Alloys.
5. F. Garofalo et al., "Creep and Creep Rupture Relationships in an Austenitic Stainless Steel," *Trans. Metall. Soc. AIME* 221: 310-19 (1961).

6. W. E. Leyda and J. P. Rowe, *A Study of Time for Departure from Secondary Creep for Eighteen Steels*, ASM Tech. Rep. P9-6.1, American Society for Metals, Metals Park, Ohio, 1969.
7. R. L. Klueh, *Creep and Rupture Behavior of Annealed 2 1/4 Cr-1 Mo Steel*, ORNL-5219 (December 1976).
8. F. Garofalo, *Fundamentals of Creep and Creep-Rupture in Metals*, Macmillan Company, New York, 1965.
9. D. A. Woodford, "Measurement and Interpretation of Stress Dependence of Creep at Low Stress," *Mater. Sci. Eng.* 4: 146-54 (1969).
10. Z. Yano, "On the Anomaly in the Nickel-Rich Solid Solution of Nickel-Chromium Binary System," *Rikagaku Kenkyusho Iho* 19: 110-17 (1940).
11. H. Thomas, "Über Widerstandslegierungen," *Z. Phys.* 129: 219-32 (1951).
12. A. Taylor and K. G. Hinton, "Study of Order-Disorder Precipitation Phenomena in Nickel-Chromium Alloys," *J. Inst. Met.* 81: 169-80 (1952).
13. H. E. McCoy, Jr. and D. L. McElroy, "Electrical Resistivity Anomaly in Nickel-Base Alloys," *ASM Trans. Q.* 61: 730-41 (1968).
14. Private communication, R. K. Williams, Oak Ridge National Laboratory.
15. J. C. Fisher, "On the Strength of Solid Solution Alloys," *Acta Metall.* 2: 9-10 (1954).
16. N. S. Stoloff and R. G. Davies, "The Mechanical Properties of Ordered Alloys," *Progress in Materials Science*, Vol 13, Pergamon Press, New York, 1966.
17. Private communication, V. K. Sikka, Oak Ridge National Laboratory.
18. J. D. Lubahn, "Simultaneous Aging and Deformation in Metals," *Trans. AIME* 182: 702-08 (1949).
19. P. A. Chalco, *Microstructure and Mechanical Properties of Cr-Mo Steel*, PhD Thesis, University of California, Los Angeles, 1974.
20. E. N. da C. Andrade, "On the Viscous Flow in Metals and Allied Phenomena," *Proc. R. Soc. London Ser. A.* 84: 1-11 (1910).

1
u

ORNL-5404
 Distribution Category
 UC-79b, -h, -k

INTERNAL DISTRIBUTION

| | | | |
|--------|-------------------------------|-----|---------------------------------|
| 1-2. | Central Research Library | 33. | H. Postma |
| 3. | Document Reference Section | 34. | C. E. Pugh |
| 4-6. | Laboratory Records Department | 35. | V. K. Sikka |
| 7. | Laboratory Records, ORNL RC | 36. | G. M. Slaughter |
| 8. | ORNL Patent Office | 37. | J. H. Smith |
| 9-13. | M. K. Booker | 38. | J. O. Stiegler |
| 14. | C. R. Brinkman | 39. | J. P. Strizak |
| 15. | J. M. Corum | 40. | R. W. Swindeman |
| 16. | D. P. Edmonds | 41. | D. B. Trauger |
| 17. | R. F. Hibbs | 42. | G. T. Yahr |
| 18-20. | M. R. Hill | 43. | R. W. Balluffi (Consultant) |
| 21-25. | J. F. King | 44. | P. M. Brister (Consultant) |
| 26-30. | R. L. Klueh | 45. | W. R. Hibbard, Jr. (Consultant) |
| 31. | H. E. McCoy, Jr. | 46. | John Moteff (Consultant) |
| 32. | J. W. McEnerney | 47. | N. E. Promisel (Consultant) |

EXTERNAL DISTRIBUTION

48-49. DOE DIVISION OF REACTOR RESEARCH AND TECHNOLOGY, Washington, DC
 20545
 Director

50-51. DOE OAK RIDGE OPERATIONS OFFICE, P.O. Box E, Oak Ridge, TN 37830
 Director, Research and Technical Support Division
 Director, Reactor Division

52-315. DOE TECHNICAL INFORMATION CENTER, Office of Information Services,
 P.O. Box 62, Oak Ridge, TN 37830
 For distribution as shown in TID-4500 Distribution Category,
 UC-79b (Fuels and Materials Engineering Development);
 UC-79h (Structural Materials Design Engineering); and
 UC-79k (Components).